Available online at www.sciencedirect.com
SCIENCE DIRECT®
Polymer 44 (2003) 5477–5495
polymer
www.elsevier.com/locate/polymer

Feature Article

Molecular properties of helical polysilylenes in solution

Takahiro Sato[a,*], Ken Terao[b,1], Akio Teramoto[b], Michiya Fujiki[c]

[a]*Department of Macromolecular Science, Osaka University and CREST of Japan Science and Technology, 1-1 Machikaneyama-cho, Toyonaka, Osaka 560-0043, Japan*

[b]*Research Organization of Science and Engineering and Faculty of Science and Engineering, Ritsumeikan University and CREST of Japan Science and Technology, Nojihigashi 1-1-1, Kusatsu, Siga 525-8577, Japan*

[c]*Graduate School of Materials Science, Nara Institute of Science and Technology (NAIST) and CREST of Japan Science and Technology, 8916-5 Takayama, Ikoma, Nara 630-0101, Japan*

Received 4 June 2003; received in revised form 26 June 2003; accepted 26 June 2003

Abstract

This article reviews recent advances in research of helical conformations of optically active polysilylenes in solution. The helical conformation induces strong circular dichroism, chain stiffness, and liquid crystallinity in polysilylene chains, and it sensitively affects electronic state in the σ-conjugated silicon backbone. The helical conformation is determined by the internal rotation potential of the silicon backbone, and it turns out that the internal potential remarkably depends on the chemical structure of side-chains bonded to polysilylenes. Interrelations among these properties, the internal potential, and the side-chain chemical structure are discussed for optically active poly(dialkylsilylene)s.

Keywords: Polysilylenes; Helical polymers; Solution properties

1. Introduction

Polysilylene derivatives can be regarded as a counterpart of vinyl polymers, of which backbones consist only of silicon atoms, instead of carbon atoms, being connected each other only with single Si–Si bonds. In spite of their simple main-chain chemical structure, polysilylenes possess various interesting molecular properties distinct from vinyl polymers [1–4]. It is well known that they have unique and interesting optical, electric, and photochemical properties owing to the σ-conjugation in the silicon backbone chains [1,5]. In addition to these properties, it has been more recently revealed that polysilylenes bearing optically active side-chains exhibit remarkable chiroptical properties, which give us the opportunity of their applications to chiral molecular switches or memories [3,4]. The strong circular dichroism arising from the silicon backbone in solution is evidence that the backbone of the optically active polysilylenes takes a helical conformation in solution.

Owing to their helical nature, global conformations of polysilylene derivatives are also very interesting. The rigidity of the chains remarkably depends on chemical structures of side-chains [6–10]. Some vinyl polymers can take helical conformations in solution, e.g. a polymethacrylate with bulky side groups [11], but their poor solubility hinders from studying the global conformations in solution. Using polysilylene derivatives, we can study the interrelation between the chain rigidity and side-chain structure. (Recently, corresponding studies were made for vinyl polymers with very long side-chains, i.e. polymacromonomers [12,13].)

Furthermore, the chain rigidity gives liquid crystallinity to polysilylenes. Recently, it was found that a polysilylene derivative possesses both lyotropic and thermotropic liquid crystallinity [10,14]. This is another property distinctive from vinyl polymers which do not exhibit liquid crystallinity unless they have mesogenic moieties [15] or very long side-chains (polymacromonomers) [16–18].

Our goal of polysilylene researches is to establish interrelations among their various properties and furthermore explain them from the first principles. The present article surveys recent advances in these researches. After

* Corresponding author. Tel./fax: +81-6-6850-5461.
E-mail address: tsato@chem.sci.osaka-u.ac.jp (T. Sato).
[1] Present address: Department of Biological and Chemical Engineering, Faculty of Engineering, Gunma University, Kiryu 376-8515, Japan.

0032-3861/03
doi:10.1016/S0032-3861(03)00574-3

describing the theoretical background and experimental procedures in Sections 2 and 3, respectively, we are concerned with optical and chiroptical properties (Section 4), global conformations (Section 5), and liquid crystallinity (Section 7) of polysilylenes. In Section 6, we try to explain the results given in Sections 4 and 5 consistently in terms of the internal rotation potential.

Recently, we have reviewed polysilylenes with variety of side-chains in another article [4]. Here we limit our arguments to poly(dialkyl silylene)s, choosing the four polysilylenes listed in Scheme 1: poly[(*R*)-3,7-dimethyloctyl-(*S*)-3-methylpentylsilylene] (PRS), poly[*n*-hexyl-(*S*)-2-methylbutylsilylene] (PH2MBS), poly[*n*-decyl-(*S*)-2-methylbutylsilylene] (PD2MBS), and poly[*n*-hexyl-(*S*)-3-methylpentylsilylene] (PH3MPS). We use the abbreviations shown in the scheme to distinguish them. In principle, we can make parallel arguments on other polysilylene derivatives.

2. Theoretical background

2.1. Geometry of helical polysilylene chains

The backbone conformation of polysilylenes is determined by bond lengths, bond angles, and internal rotation angles about Si–Si bonds. Changes in the bond length and bond angle are so small in usual conditions that they play only minor roles in arguments of the polymer conformation. In the following, we consider the effect of the change in the internal rotation angle on the helical conformation, keeping the backbone bond length and bond angle to be 0.235 nm and 111°, respectively [5].

The backbone conformation of a polysilylene chain with the degree of polymerization N_0 (or $N_0 - 1$ main-chain bonds) can be specified by the set of internal rotation angles $\{\tilde{\phi}_k : 1 \le k \le N_0 - 1\}$. When all the rotational angles take an identical value, the polysilylene chain becomes a helix. It was reported that poly[(di-*n*-butyl)silylene] and poly[(di-*n*-pentyl)silylene] form a 7/3 helix in the crystalline state [1,19], where three turns of the helix consist seven repeating units. The internal rotational angle in those helical polysilylene chains deviates from the *trans* state by 31.3°, and the helix pitch h per repeating unit is calculated to be 0.19 nm using the above bond length and bond angle.

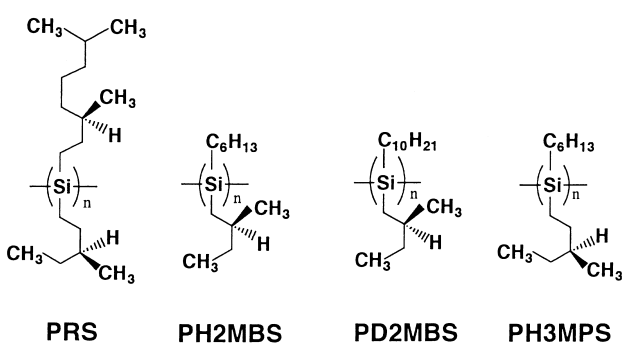

Scheme 1. Chemical structures of optically active polysilylenes discussed in this article.

For the polyethylene chain, it is well known that each methylene unit can essentially take three different rotational isomeric states: the *trans*, *gauche*, and *gauche prime* states. When all the methylene units are in the *trans* state, the chain takes the *trans* zig-zag conformation (which may be regarded as a 2/1 helix), while the chain taking the all *gauche* (or *gauche prime*) conformation becomes a 4/1 helix. On the other hand, in the case of poly(tetrafluoroethylene), the *trans* state causes steric hindrance between bulky fluorine atoms attaching to the second nearest carbon atoms along the main-chain, which makes the *trans* zig-zag conformation unstable [20]. As a result, the poly(tetrafluoroethylene) chain forms a 13/6 or 15/7 helix in crystalline state [21], where the rotational angle of each unit deviates from the *trans* state by ca. 15°. Similarly, the 7/3 helix of the above-mentioned polysilylenes may arise from steric hindrance between side-chains attaching to the second nearest silicon atoms in the backbone (cf Fig. 1). The distance between the two side-chains increases by rotations about successive two bonds in the same direction from the *trans* states as depicted in panels B and C of Fig. 1. The steric hindrance among neighboring side-chains may also prohibit the *gauche* and *gauche prime* states, if the side-chain is bulky enough. In what follows, we assume that the *gauche* and *gauche* prime states are completely prohibited for helical polysilylenes.

We define the internal rotation angle $\tilde{\phi}_k$ as the dihedral angle between two planes defined by neighboring bonds $k-1$ and k, and k and $k+1$, respectively, measured relative to the *trans* conformation and being positive at the clockwise rotation about bond k in view from the bond $k-1$ side. It is noted that the conventional rotation angle ϕ_k is measured relative to the *cis* conformation so that $\tilde{\phi}$ is equal to $\phi_k - 180°$. The polysilylene chain where all the internal rotation angles $\tilde{\phi}$ are equal to 31.3° is the perfect left-handed 7/3 helix and that with $\tilde{\phi} = -31.3°$ is the perfect right-handed one. In solution, two kinds of disorder may be introduced in the perfectly helical polysilylene chain: the torsional fluctuation and the helix reversal. Thermal agitation by surrounding solvent molecules induces a more or less deviation of each internal rotation angle in the helical polysilylene chains from the most energetically stable state. This torsional fluctuation will be discussed in the following subsection. In addition to this, the polysilylene chain may drastically change $\tilde{\phi}$ from $+31.3°$ to $-31.3°$ or its helical sense along the chain. The boundary between the helical portions of opposite sense is another disorder or defect of the chain. The chain may kink at this helix reversal point.

If the internal rotational angle suddenly changes from $+31.3°$ to $-31.3°$ along the chain without some intermediate rotational state (the *two-state approximation*), we can calculate the kink angle $\hat{\theta}_V$ formed by helix axes in both

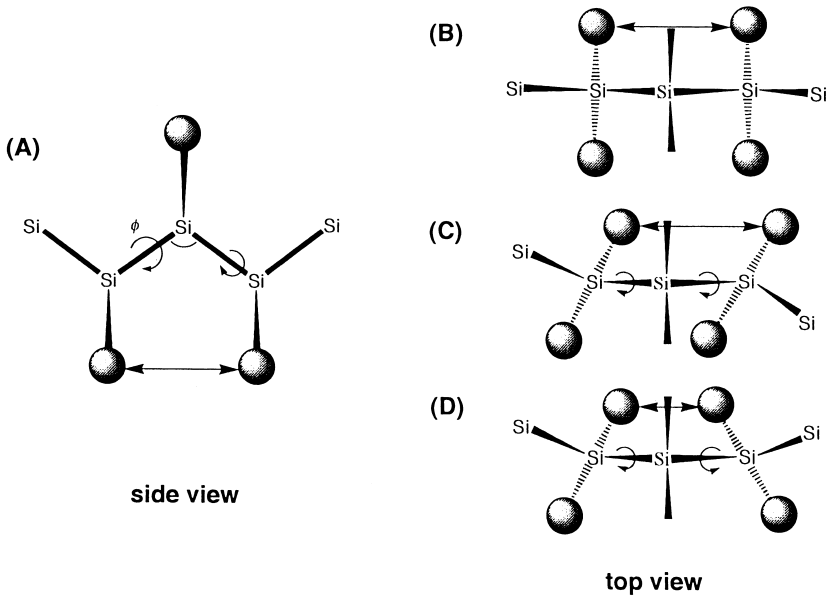

Fig. 1. Schematic diagrams of a polysilylene chain with two successive bonds in the trans state (B), rotating in the same direction (C), and rotating in the opposite direction (D) from the trans state.

sides of the reversal point to be 18°, which is not so large angle. However, the two state approximation may not always hold, but the helix reversal could consist of few repeating units taking rotation angles other than ±31.3°. For example, Lifson et al. [22] demonstrated by an empirical force field calculation of polyisocyanates that two or three repeating units take some intermediate conformations other than the right- nor left-handed helical conformations in the helix reversal region. Unfortunately, such a force field calculation has not been performed for polysilylene chains.

For helical polysilylene chains, it is known that the helix reversal does not easily take place (cf. Section 4.2). Difficulty of the helix reversal is also explained by steric hindrance between side-chains attaching to the second nearest silicon atoms in the backbone. If the sequential internal rotation angles $\tilde{\phi}_{k-1}$ and $\tilde{\phi}_k$ are +31.3° and −31.3°, respectively, the side-chains under consideration come even closer than the all *trans* state as schematically shown in Fig. 1D. To be released from this steric hindrance, the polysilylene chain may take some intermediate conformation with higher free energy than the helical ones at the helix reversal. Thus the helix reversal costs excess free energy ΔG_r per mole of monomer unit and its probability can be calculated by $\exp(-\Delta G_r/RT)$. where RT is the gas constant multiplied by the absolute temperature.

2.2. Torsional fluctuation

The torsional fluctuation is usually expressed in two ways. One is the Gaussian approximation. Assuming the Gaussian statistics, one writes the population of the rotational angle $\tilde{\phi}$ about each bond in a helical polymer chain by [23]

$$P(\tilde{\phi}) = \frac{1}{\sqrt{2\pi\langle(\tilde{\phi}-\tilde{\phi}_0)^2\rangle}}\exp\left[-\frac{(\tilde{\phi}-\tilde{\phi}_0)^2}{2\langle(\tilde{\phi}-\tilde{\phi}_0)^2\rangle}\right] \tag{2.1}$$

where $\tilde{\phi}_0$ is the average rotation angle and $\langle(\tilde{\phi}-\tilde{\phi}_0)^2\rangle^{1/2}$ is the standard deviation of $\tilde{\phi}$. The other is to assume some specific internal potential $E(\tilde{\phi})$. According to the Boltzmann distribution, $P(\tilde{\phi})$ is given by

$$P(\tilde{\phi}) = \frac{\exp[-E(\tilde{\phi})/RT]}{\int \exp[-E(\tilde{\phi})/RT]\mathrm{d}\tilde{\phi}} \tag{2.2}$$

where $E(\tilde{\phi})$ expresses the potential energy per mole of repeating unit (or Si–Si bond) and the integration range in the denominator is from 0 to π (for the left-handed helix) or from −π to 0 (for the right-handed helix). The standard deviation is calculated by

$$\langle(\tilde{\phi}-\tilde{\phi}_0)^2\rangle = \frac{\int(\tilde{\phi}-\tilde{\phi}_0)^2\exp[-E(\tilde{\phi})/RT]\mathrm{d}\tilde{\phi}}{\int \exp[-E(\tilde{\phi})/RT]\mathrm{d}\tilde{\phi}} \tag{2.3}$$

Sato et al. [24] proposed the following equation to express $E(\tilde{\phi})$ for helical polysilylene chains:

$$E(\tilde{\phi}) = E_T - C + C\,\mathrm{e}^{-(\tilde{\phi}_0/\beta)^2}(\tilde{\phi}/\beta)^2 + C\,\mathrm{e}^{-(\tilde{\phi}/\beta)^2} \tag{2.4}$$

where

$$C \equiv \frac{E_T - E_0}{1-[1+(\tilde{\phi}_0/\beta)^2]\mathrm{e}^{-(\tilde{\phi}_0/\beta)^2}} \tag{2.5}$$

and E_T and E_0 are potential energies at $\tilde{\phi}=0$ (the *trans*-conformation) and $\tilde{\phi}_0$ (the potential-minimum angle), respectively, and β is a parameter relating the steepness of the well.

For optically active polysilylenes, the mirror image of

the right-handed helix is not identical with the left-handed helix due to chiral pendant groups. Due to this dissymmetry, the internal potential $E(\tilde{\phi})$ is not an even function of $\tilde{\phi}$ for optically active polysilylenes, so that the parameters in Eqs. (2.4) and (2.5) (E_0, $\tilde{\phi}_0$, and β) should take different values in the positive and negative $\tilde{\phi}$ regions. In what follows, E_0, $\tilde{\phi}_0$, and β at $\tilde{\phi} < 0$ are denoted as $E_{0,P}$, $\tilde{\phi}_{0,P}$, and β_P, those at $\tilde{\phi} > 0$ as $E_{0,M}$, $\tilde{\phi}_{0,M}$, and β_M, and helices with the negative and positive $\tilde{\phi}$ are referred to as the P-helix and M-helix, respectively. We select the arithmetic average of $E_{0,P}$ and $E_{0,M}$ as the reference energy, so that $E_{0,P}$ is equal to $-E_{0,M}$.

2.3. Statistical mechanics of helical chains

If the internal potential is double well-like as given by Eq. (2.4), each repeating unit (or Si–Si bond) in the polymer chain takes either P- or M-helical state, and the whole chain conformation can be specified by a sequence of the two states. Using $E(\tilde{\phi})$ given by Eq. (2.4), statistical weights of the repeating unit in the P- and M-helical states may be calculated by

$$u_P = \int_{-\pi}^{0} \exp[-E(\tilde{\phi})/RT]\mathrm{d}\tilde{\phi}, \qquad u_M = \int_{0}^{\pi} \exp[-E(\tilde{\phi})/RT]\mathrm{d}\tilde{\phi} \tag{2.6}$$

and the free energy difference $2\Delta G_h$ between the M- and P-helical states (per mole of the repeating unit) is defined by

$$\frac{u_M}{u_P} = \exp(-2\Delta G_h/RT) \tag{2.7}$$

For achiral polysilylenes, u_P and u_M are identical, so that ΔG_h is equal to zero.

Let us calculate the conformational partition function Z_{N_0} of the helical polysilylene chain with the degree of polymerization N_0. The definition of the helix sense needs at least three bonds, and the partition function Z_4 of the tetramer is given by $u_P + u_M$. For the pentamer, we have four different conformations, PP, PM, MP, and MM. As mentioned in Section 2.1, the helix reversal in the PM and MP conformations costs excess free energy ΔG_r, so that the statistical weight of those conformations is written as $u_P u_M \upsilon$, where υ is the statistical weight of the helix reversal given by

$$\upsilon = \exp(-\Delta G_r/RT) \tag{2.8}$$

Thus the partition function Z_5 reads $u_P^2 + 2u_P u_M \upsilon + u_M^2$. Just similarly, we can formulate Z_{N_0} for higher N_0. Using the matrix method, it can be formally written as

$$Z_{N_0} = \begin{pmatrix} u_P & u_M \end{pmatrix} \begin{pmatrix} u_P & \upsilon u_M \\ \upsilon u_P & u_M \end{pmatrix}^{N_0-4} \begin{pmatrix} 1 \\ 1 \end{pmatrix} \tag{2.9}$$

Lifson et al. [25] calculated the partition function by the sequence generating function method. This method does not need tedious matrix calculations in Eq. (2.9) and is more convenient to calculate Z_{N_0}. Their result is written as

$$Z_{N_0} = x_+^{N_0}\left(1 + \upsilon \Big/ \sqrt{\frac{1}{4}(u_P - u_M)^2 + \upsilon^2}\right) + x_-^{N_0}\left(1 - \upsilon \Big/ \sqrt{\frac{1}{4}(u_P - u_M)^2 + \upsilon^2}\right) \tag{2.10}$$

where

$$x_\pm \equiv \frac{1}{2}(u_P + u_M) \pm \sqrt{\frac{1}{4}(u_P - u_M)^2 + \upsilon^2} \tag{2.11}$$

Average numbers of repeating units in the P- and M-states expected in a polysilylene chain of the degree of polymerization N_0 can be calculated from Z_{N_0} by

$$n_P = \frac{\mathrm{d}\ln Z_{N_0}}{\mathrm{d}\ln u_P}, \qquad n_M = \frac{\mathrm{d}\ln Z_{N_0}}{\mathrm{d}\ln u_M} \tag{2.12}$$

and also the average number of helix reversals in the chain by

$$n_V = \frac{\mathrm{d}\ln Z_{N_0}}{\mathrm{d}\ln \upsilon} \tag{2.13}$$

The expected fraction f_P of the repeating unit taking the P-state can be calculated by

$$f_P = n_P/(n_P + n_M) \tag{2.14}$$

and the enantiomer excess is given by $2f_P - 1 = (n_P - n_M)/(n_P + n_M)$. Lifson et al. [25] proposed a useful approximated equation for $2f_P - 1$ (cf Eq. (23) in their paper). Since each helical sequence other than the first one in the chain is initiated by a single helix reversal, the average number of P- or M-sequences is equal to $(n_V + 1)/2$, and average numbers l'_P and l'_M of repeating units in a P- and M-sequence can be calculated by n_P and n_M, respectively, divided by $(n_V + 1)/2$. For an infinitely long chain, the arithmetic mean of l'_P and l'_M is given in a good approximation by

$$\langle l' \rangle = \sqrt{\frac{1}{4}(u_P - u_M)^2 + \upsilon^2} \Big/ \upsilon^2 \tag{2.15}$$

In the above formulation of Z_{N_0}, we did not consider possible intermediate rotational states of bonds other than the P- nor M-states at the helix reversal (the two-state approximation). However, because the helix reversal is a rare event in the polysilylene chain, this is a good approximation in the calculations of f_P and $\langle l' \rangle$.

2.4. Persistence length of helical polymers

Let us first consider a P-helical polysilylene chain with no helix reversal. The internal rotation angle $\tilde{\phi}$ of each repeating unit in the chain fluctuates around the potential-minimum angle $\tilde{\phi}_{0,P}$. If the fluctuation of all $\tilde{\phi}$ takes place independently, the characteristic ratio for the chain at sufficiently high degree of polymerization can be written as

[26,27]

$$C_{\infty,\mathrm{P}} = \left(\frac{1+\cos\hat{\theta}}{1-\cos\hat{\theta}}\right)\frac{(1+\langle\cos\tilde{\theta}\rangle_{\mathrm{P}})^2+\langle\sin\tilde{\phi}\rangle_{\mathrm{P}}^2}{1-\langle\cos\tilde{\theta}\rangle_{\mathrm{P}}^2-\langle\sin\tilde{\phi}\rangle_{\mathrm{P}}^2} \tag{2.16}$$

where $\hat{\theta}$ is the complimentary angle of the Si–Si–Si bond angle and $\langle\cdots\rangle_{\mathrm{P}}$ represents the thermal average over the fluctuation of $\tilde{\phi}$. Using the internal potential, we write the averages $\langle\cos\tilde{\phi}\rangle_{\mathrm{P}}$ and $\langle\sin\tilde{\phi}\rangle_{\mathrm{P}}$ by

$$\langle\cos\tilde{\phi}\rangle_{\mathrm{P}} = \frac{1}{u_{\mathrm{P}}}\int_{-\pi}^{0}\cos\tilde{\phi}\exp[-E(\tilde{\phi})/RT]\mathrm{d}\tilde{\phi},$$
$$\langle\sin\tilde{\phi}\rangle_{\mathrm{P}} = \frac{1}{u_{\mathrm{P}}}\int_{-\pi}^{0}\sin\tilde{\phi}\exp[-E(\tilde{\phi})/RT]\mathrm{d}\tilde{\phi} \tag{2.17}$$

On the other hand, $C_{\infty,\mathrm{P}}$ is written in terms of the wormlike chain model as [27,28],

$$C_{\infty,\mathrm{P}} = 2q_{0,\mathrm{P}}h/b^2 \tag{2.18}$$

where $q_{0,\mathrm{P}}$ is the persistence length of the P-helix, h is the helix pitch per the repeating unit, and b is the Si–Si bond length. Combining Eqs. (2.16) and (2.18), we have

$$q_{0,\mathrm{P}} = \frac{b^2}{2h}\left(\frac{1+\cos\hat{\theta}}{1-\cos\hat{\theta}}\right)\frac{(1+\langle\cos\tilde{\phi}\rangle_{\mathrm{P}})^2+\langle\sin\tilde{\phi}\rangle_{\mathrm{P}}^2}{1-\langle\cos\tilde{\phi}\rangle_{\mathrm{P}}^2-\langle\sin\tilde{\phi}\rangle_{\mathrm{P}}^2} \tag{2.19}$$

If there is no fluctuation in $\tilde{\phi}$, $\langle\cos\tilde{\phi}\rangle_{\mathrm{P}}^2+\langle\sin\tilde{\phi}\rangle_{\mathrm{P}}^2$ is equal to unity so that $q_{0,\mathrm{P}}$ becomes infinity. The fluctuation of $\tilde{\phi}$ reduces $q_{0,\mathrm{P}}$ to a finite value. Replacing $\langle\cdots\rangle_{\mathrm{P}}$ by $\langle\cdots\rangle_{\mathrm{M}}$ in Eq. (2.19), we can obtain the persistence length $q_{0,\mathrm{M}}$ of the M-helix.

Next, we consider the effect of helix reversals on the persistence length. As mentioned in Section 2.1, the reversal points may cause kinks and the chain may not be regarded as a *regular* wormlike chain. In 1986, Mansfield [29] proposed the broken wormlike chain (BWC) model, which may be suitable to describe helical polymer chains with helix reversals. If P- and M-helical portions possess different stiffness, the BWC can be defined as a continuous limit of a freely rotating chain with three different types of bond angles, corresponding to the P- and M-helix portions and the helix reversal. The resulting *effective* persistence length q of the BWC is given by

$$\frac{1}{q} = \frac{f_{\mathrm{P}}}{q_{0,\mathrm{P}}} + \frac{1-f_{\mathrm{P}}}{q_{0,\mathrm{M}}} + \frac{1-\cos\hat{\theta}_{\mathrm{V}}}{\langle l\rangle} \tag{2.20}$$

where $\hat{\theta}_{\mathrm{V}}$ is the kink angle at the helix reversal and $\langle l\rangle$ is the arithmetic mean of average lengths of a P- and M-sequence on an infinitely long chain, i.e. $\langle l'\rangle = h\langle l'\rangle$ where $\langle l'\rangle$ is given by Eq. (2.15). The quantity $\langle l\rangle$ is sometimes referred to as the 'helical persistence length' in literature, but it should be distinguished from q, because the contribution of the third term on the right-hand side of Eq. (2.20) is often minor [25].

Mansfield [29] demonstrated that the mean-square end-to-end distance and radius of gyration of the BWC are identical with those of the original wormlike chain with the persistence length being equal to q given by Eq. (2.20), and the difference appears in the fourth and higher moments of the end-to-end distance R. Employing the Koyama distribution function for R [30], Mansfield calculated the mean reciprocal end-to-end distance $\langle R^{-1}\rangle$ of the BWC as a function of q, the contour length L, and the parameter δ defined by

$$\delta \equiv \frac{q}{2\langle l\rangle}(1-\cos\hat{\theta}_{\mathrm{V}})^2 \tag{2.21}$$

The parameter δ is equal to $|(\lambda_2-\lambda_1)/\lambda_1|$ in the original paper [29], and at $\delta = 0$, the kink contribution disappears in the BWC. According to his result, if $\delta \leq 0.3$, $\langle R^{-1}\rangle$ of the BWC is equal to that of the original wormlike chain within 3.5% error for any q and L. Thus we can expect that the intrinsic viscosity and hydrodynamic radius of the BWC, which are calculated from the mean reciprocal distance between any two contour points on the BWC, are indistinguishable from those of the regular wormlike chain, if δ is small enough. Dilute solution properties of helical polymers have been so far analyzed in terms of the regular wormlike chain model to obtain q [7,8,10,9,31–33], and the resulting q may be identified with that of the BWC in most of cases where δ is small enough.

2.5. Electronic states of polysilylene chains

Polysilylenes are known as σ-conjugated polymers or quasi-one-dimensional semiconductors exhibiting interesting optical and electro-optical properties. In the chains, sp^3 atomic orbitals protruded from adjacent Si atoms strongly overlap, and the bonding and unbonding states of the sp^3 orbitals are incorporated to provide the highest occupied and the lowest unoccupied molecular orbital bands. It was shown that the band structure of the polysilane chain strongly depends on the coplanarity of the σ-bonds [34–36]. This indicates that the optical absorption spectrum of polysilylene chains depends on the backbone conformation. In fact, poly(dialkyl silylene)s taking different helical conformations in solid state exhibits different absorption spectra [35,36].

Abe et al. [36–38] performed a quantum-mechanical calculation using a one-dimensional exciton model including long-range Coulomb interactions between electron and lattice and also between electrons in the chain. The absorption spectrum they obtained quite resembles experimental one for polysilylenes. Furthermore, Abe et al. [38–40] introduced a lattice fluctuation in his model and demonstrated that the exciton absorption significantly weakens and broadens with increasing the degree of fluctuation. Although the lattice fluctuation in his one-dimensional model cannot be directly related to the polysilylene backbone conformation, his result indicates that the optical absorption spectrum depends on some disorder in the backbone conformation of polysilylenes.

3. Experimental section

Poly(dialkylsilylene)s were prepared by the Wurtz-type condensation of the corresponding dichlorodiorganosilane with sodium in an inert solvent. Polymerized samples were divided into a number of fractions of considerably narrow molecular weight distributions by fractional precipitation or by SEC; the ratio of the z-average to weight-average molecular weights usually less than 1.2 [8,9].

Weight-average molecular weights M_w of fractionated samples were determined in isooctane by sedimentation equilibrium or light scattering [8,10]. The apparent molecular weight estimated by SEC with a calibration curve constructed using standard polystyrene samples considerably overestimates M_w in a high molecular weight region; the apparent molecular weight of a high molecular-weight PD2MBS sample was five times as high as M_w [41].

Intrinsic viscosities $[\eta]$ and z-average radii of gyration $\langle S^2\rangle_z^{1/2}$ of fractionated polysilylene samples were measured in isooctane by viscometry and light scattering, respectively, [8]. Viscosity measurements of very high molecular weight samples were made with a four-bulb low-shear rate capillary viscometer, and $[\eta]$ were determined by extrapolation to the zero shear rate. Second virial coefficients of the samples in isooctane were estimated by light scattering and/or sedimentation equilibrium.

The circular dichroism (CD) and ultraviolet absorption (UV) of isooctane solutions of fractionated polysilylene samples were measured with a quartz cell of 0.5 cm path length at wavelengths between 260 and 360 nm [42]. Concentrations of test solutions were chosen so as to give absorbency at the peak between 0.8 and 1.5. To avoid the photodegradation of the samples during the measurements, different solutions were used at each temperature.

4. Optical and chiroptical properties [42,9]

4.1. Experimental results

Fig. 2 shows the CD and UV spectra of a PH3MPS sample ($M_w = 51.0 \times 10^4$) in isooctane at the indicated temperatures. It is seen that both curves have a sharp absorption peak centered at wavelength $\lambda \approx 320$ nm, and change their shapes with temperature. The strong CD signal at low temperatures demonstrates that the Si backbone of this polysilylene takes some helical conformations and furthermore the population of the enantiomeric helical conformations is uneven. However, the CD signal almost disappears at 25 °C. The peak height of the UV spectrum also decreases with increasing temperature, but it does not tend to zero even at 25 °C.

The molecular weight dependencies of the CD and UV spectra for PH3MPS in isooctane are shown in Fig. 3 (at −75 °C). While both CD and UV curves for high molecular weight samples (F12, F32, and F42) overlap each other, the

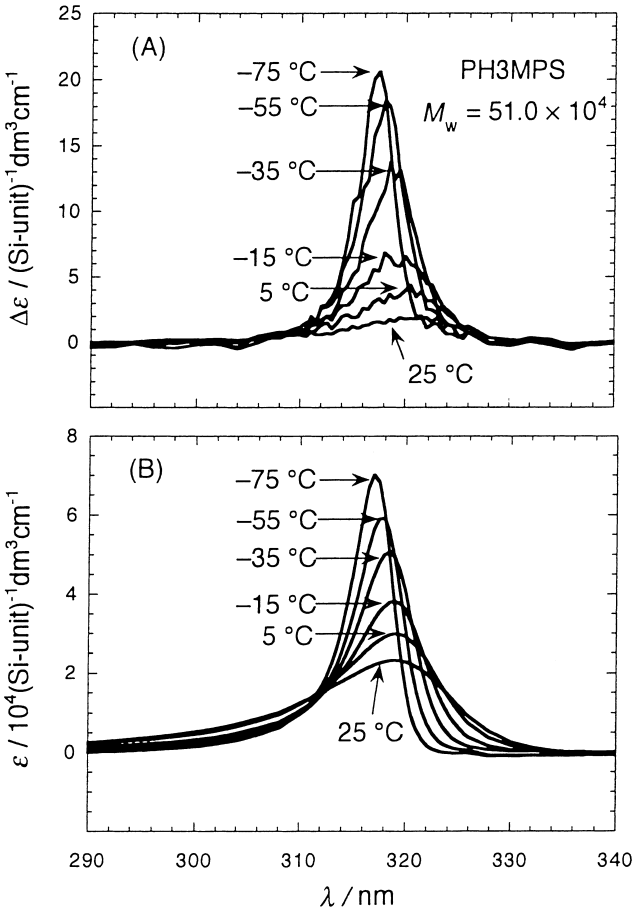

Fig. 2. CD and UV spectra of a PH3MPS sample ($M_w = 51.0 \times 10^4$, $N_0 = 2570$) in isooctane at the indicated temperatures.

peak heights of both curves diminish along with decreasing the molecular weight. The change of the CD curve is more rapid than that of the UV.

The magnitude of an absorption band is usually characterized by the dipole strength D calculated from the molar absorption coefficient ε by [43,44]

$$D = \frac{3 \ln 10 \tilde{c} \varepsilon_0 \hbar}{\pi N_A} \int_{\lambda_{min}}^{\lambda_{max}} \frac{\varepsilon}{10\lambda} d\lambda \tag{4.1}$$

where $\tilde{c}$ is the velocity of light, ε_0 is the permittivity of vacuum, $\hbar$ is the Planck constant divided by 2π, and N_A is the Avogadro constant. (To transform the units of ε from the conventional to the SI units, ε in the integral is divided by 10.) For polysilylene derivatives, we choose λ_{min} and λ_{max} to be 270 and 340 nm, respectively, in most cases. The dipole strength is equal to the square of the electric dipole transition moment which can be calculated from first principles. As shown in Fig. 4 by unfilled circles, D for PH3MPS is almost independent of temperature and degree of polymerization N_0, though it slightly decreases at very low N_0.

On the other hand, the basic quantity of the CD spectrum

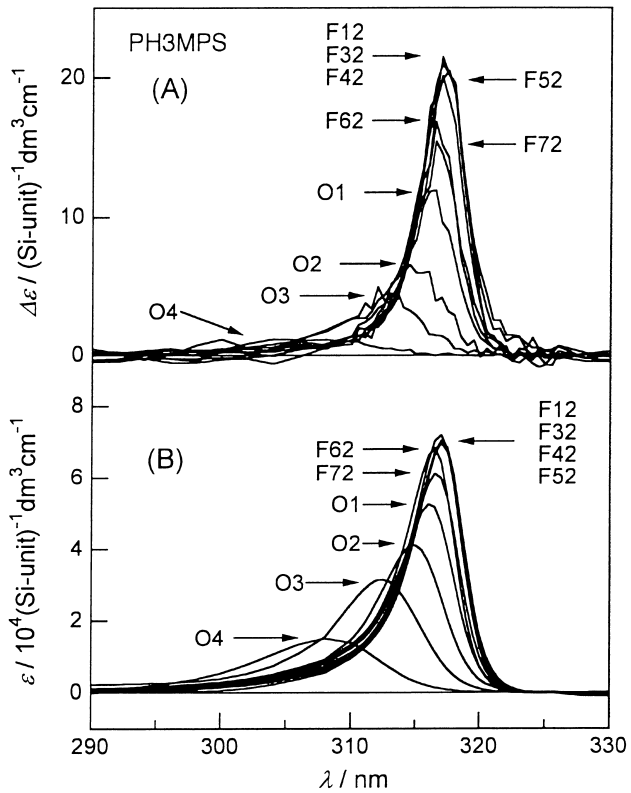

Fig. 3. Molecular weight dependencies of the CD and UV spectra for PH3MPS in isooctane at −75 °C: $N_0 = 4400$ (F12), 2570 (F32), 1290 (F42), 635 (F52), 333 (F62), 185 (F72), 103 (O1), 55.4 (O2), 34.5 (O3), and 15.5 (O4) [42].

is the rotational strength R' calculated by [43,44]

$$R' = \frac{3 \ln 10 \tilde{c} \varepsilon_0 \hbar}{4\pi N_A} \int_{\lambda_{min}}^{\lambda_{max}} \frac{\Delta\varepsilon}{10\lambda} d\lambda \qquad (4.2)$$

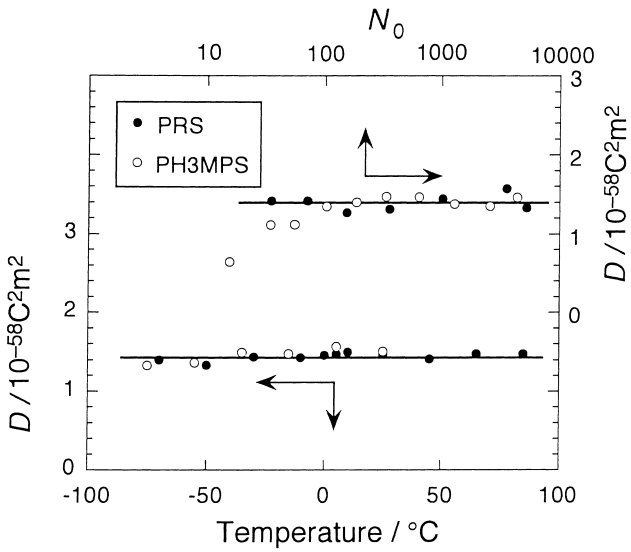

Fig. 4. Temperature and degree of polymerization dependencies of the dipole strength D for PH3MPS and PRS in isooctane calculated by Eq. (4.1). The temperature dependence is examined by a PH3MPS sample with $N_0 = 2570$ and a PRS sample with $N_0 = 1020$, while the N_0 dependence is examined at −75 °C (PH3MPS) and −30 °C (PRS).

Theoretically, it is defined as the product of the electric and magnetic transition moment vectors. The ratio $4R'/D$ is referred to as the Kuhn dissymmetry factor, and can be used as a measure of molecular chirality. Though the estimates of D and R' need integrations, we can simply estimate the dissymmetry factor g_{abs} from the ratio of the peak heights of CD and UV curves for PH3MPS, because we can overlap the two curves at each temperature and each molecular weight by multiplying a factor. Fig. 5 displays temperature and N_0 dependencies of g_{abs} for PH3MPS.

If an optically active small molecule or (electronically independent) unit in a polymer chain has a single chromophore, takes a single conformation, and its electronic moments are insensitive to nuclear displacements (or molecular vibrations and torsions), its CD and UV exhibit the following characteristic features [45]: (1) the CD and UV curves have the identical shape; (2) D and R' are characteristic to the molecule or repeating unit, being independent of the temperature, solvent condition, and degree of polymerization. The results shown in Figs. 2–4 exemplify the above features, but R' given in Fig. 5 does not exhibit the feature (2). This indicates that the repeating unit of PH3MPS takes either of enantiomeric right-handed and

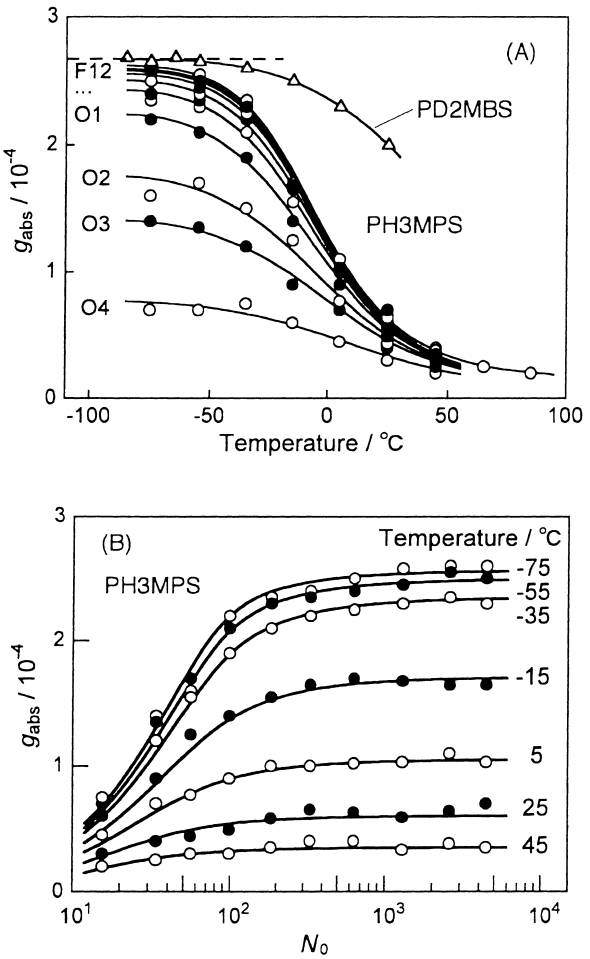

Fig. 5. (A) Temperature and (B) N_0 dependencies of the Kuhn dissymmetry factor g_{abs} for PH3MPS in isooctane [42].

left-handed helical conformations, because the enantiomeric conformations possess the same D but R' with the opposite sign. Thus the changes in R' or g_{abs} with temperature and N_0 can be ascribed to variations of the enantiomer excess of the right- and left-handed helical conformations. In other words, we can estimate from g_{abs} the enantiomer excess of the polysilylene repeating unit in solution.

From the above argument, the results of g_{abs} shown in Fig. 5 demonstrate that the enantiomer excess of the PH3MPS repeating unit sharply diminish with increasing temperature or lowering N_0 to approach to the racemic state. The temperature dependence becomes stronger with increasing N_0. Similar temperature and N_0 dependencies of the enantiomer excess were observed previously for stereospecifically deuterated poly(*n*-hexyl isocyanate)s by Green et al. [25,46–48]. In Fig. 5A, triangles indicate g_{abs} for a PD2MBS sample ($M_w = 1.2 \times 10^6$) in 25 °C isooctane. For this polysilylene, g_{abs} maintains high values or enantiomer selectivity persists up to higher temperatures. On the other hand, g_{abs} of PH3MPS with high M_w catches up that of PD2MBS at low temperature limit, which indicates that the level-off value ($= 2.7 \times 10^{-4}$) corresponds to the limit of the enantiomer excess.

Fig. 6 shows the CD and UV spectra of a PRS sample with $M_w = 2.6 \times 10^5$ in isooctane at the indicated temperatures. The temperature dependence of the UV spectrum is quite similar to that for PH3MPS shown in Fig. 2, but the CD spectrum changes its sign from negative to positive with decreasing temperature. Similarity of the CD and UV curves and also constancy of the dipole strength D are maintained irrespective of temperature and N_0 just like for PH3MPS as shown by filled cricles in Fig. 4, so that we may estimate the enantiomer excess from g_{abs} for this polysilylene too.

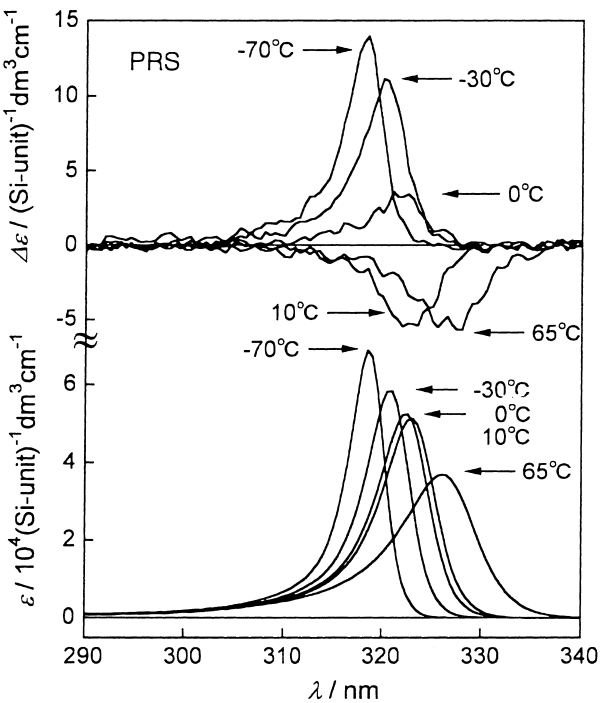

Fig. 6. CD and UV spectra of a PRS sample with $M_w = 2.6 \times 10^5$ ($N_0 = 1020$) in isooctane at the indicated temperatures [9].

The temperature dependence of g_{abs} are shown in Fig. 7. The critical temperature where g_{abs} becomes zero is common for every samples in isooctane (ca. 3 °C), but the change in the vicinity of the critical temperature is sharper for higher N_0 samples. The change of the g_{abs} sign indicates that the preferred helical sense of PRS is thermally inverted at this critical temperature. A molecular mechanical calculation for PRS implies that the right-handed helical conformation is more stable at low temperature [6]. Thus, we tentatively assume that the positive g_{abs} corresponds to the right-handed helical state (P-state) of PRS.

As shown in Fig. 8, the values of g_{abs} are almost independent of molecular weight in the range $N_0 > 10^3$, but their absolute values for lower molecular weight samples decrease significantly with decreasing N_0. The asymptotic value in the low temperature and high N_0 limits is 2.0×10^{-4}, which is slightly smaller than the corresponding value for PH3MPS and PD2MBS mentioned above. The molecular weight dependencies shown in Figs. 5B and 8 are key characteristics in order to discuss thermodynamic parameters ΔG_h and ΔG_r for the helical structure of PH3MPS and PRS in isooctane, which will be discussed in the following subsection.

Fig. 9 compares g_{abs} of PRS dissolved in three different solvents, *n*-heptane, methylcyclohexane, and 2,2,4,4,6,8,8-heptamethylnonane. The critical temperature changes with the bulkiness of the solvents. This indicates that ΔG_h is strongly dependent on the solvent bulkiness. On the other hand, we observed essentially no solvent dependence of g_{abs} for PH3MPS [42].

Although the dipole strength is essentially independent of the temperature and N_0 as shown in Fig. 4, the shape of

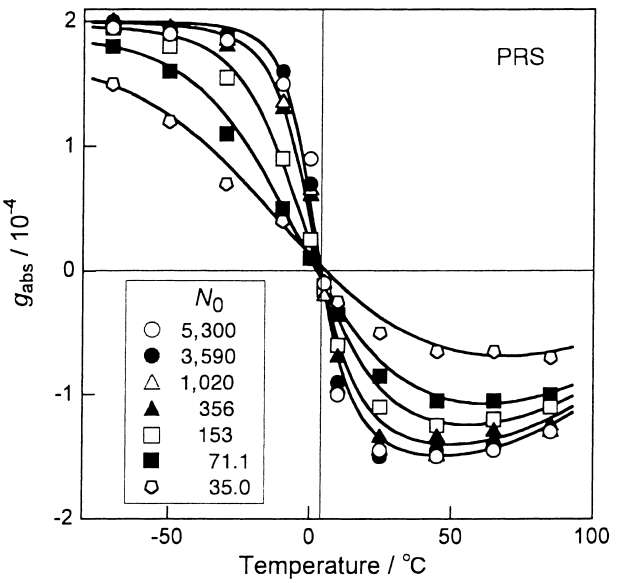

Fig. 7. Temperature dependence of g_{abs} for PRS in isooctane [9].

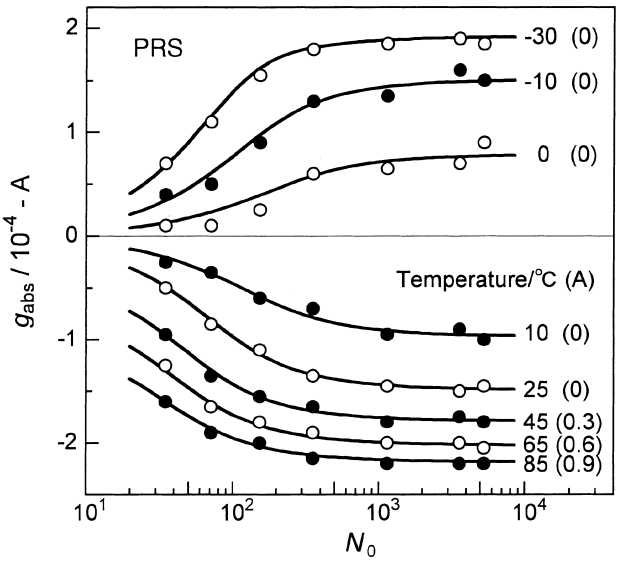

Fig. 8. N_0 dependence of g_{abs} for PRS in isooctane [9].

the UV curve itself are remarkably temperature and N_0 dependent. The shape of the spectrum can be characterized by the wavelength of the peak (λ_{max}), the peak height (ε_{max}), and the full width at half-maximum (fwhm). The N_0 dependencies of these quantities for PH3MPS at 25 and −75 °C are illustrated in Fig. 10A–C. It is seen that these quantities are independent of N_0 at $N_0 > 300$, but sharply change below that N_0. The asymptotic values of λ_{max}, ε_{max}, and fwhm at large N_0 are plotted against temperature in Fig. 10D; the subscript ∞ indicates the asymptotic values. The broadening of the spectrum with increasing temperature reflects on both $\varepsilon_{max,\infty}$ and $fwhm_\infty$, but $\lambda_{max,\infty}$ is almost independent of temperature.

The temperature and molecular weight dependencies of the UV spectrum for PRS were similar to those for PH3MPS. However, the temperature dependencies of $\varepsilon_{max,\infty}$ and $fwhm_\infty$ for high molecular weight PRS were weaker than those for PH3MPS in Fig. 10D [9]. The shape

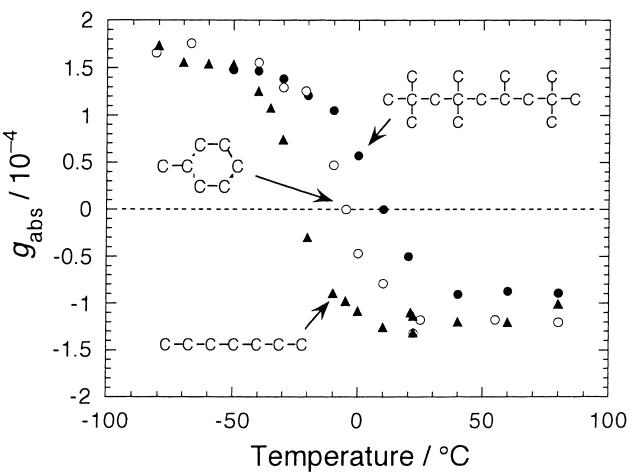

Fig. 9. Comparison of g_{abs} for PRS dissolved in three different solvents [6].

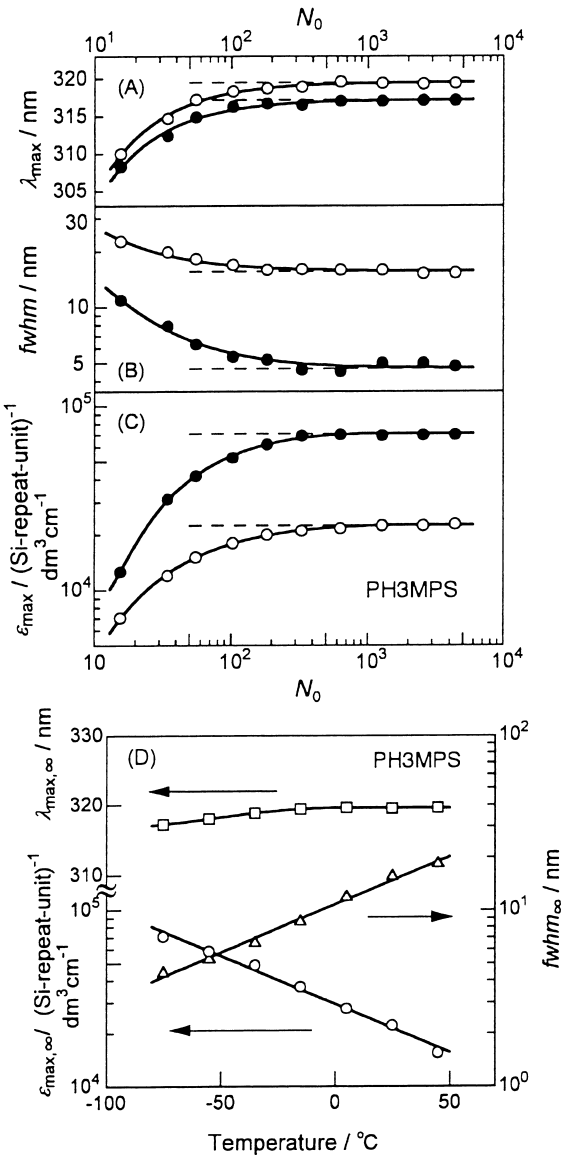

Fig. 10. N_0 dependencies of (A) peak wavelength λ_{max}, (B) the full width at half-maximum fwhm, and (C) the peak height ε_{max} of UV spectra for PH3MPS in isooctane at 25 °C (unfilled circles) and −75 °C (filled circles), and (D) temperature dependencies of the asymptotic values at high N_0, $\lambda_{max,\infty}$ (squares), $fwhm_\infty$ (triangles), and $\varepsilon_{max,\infty}$ (circles) [42].

of the UV spectra for PRS and PH3MPS will be discussed in Section 6.

4.2. Thermodynamic parameters for the helical conformation

As mentioned above, we can assume that the repeating units of polysilylene chains taking the right-handed (P) and left-handed (M) helical conformations have the same absolute values of the dipole and rotational strengths D and R' but opposite sign of R'. In such a case, we can relate g_{abs} to the fraction f_P of the repeating unit taking the P-state

by

$$g_{abs} = g_P(2f_P - 1) = g_P \frac{n_P - n_M}{n_P + n_M} \quad (4.3)$$

where g_P is the Kuhn dissymmetry factor of the repeating unit taking the P-state.

We may take the asymptotic value of g_{abs} in the low temperature and high N_0 limits as g_P : 2.7×10^{-4} for PH3MPS and 2.0×10^{-4} for PRS. Using these values of g_P as well as g_{abs} data as given in Figs. 5, 7, and 8, we obtain f_P as functions of N_0 and temperature. On the other hand, if ΔG_h and ΔG_r are given, f_P can be calculated using Eqs. (2.10)–(2.12) and (2.14) in Section 2.3 or Lifson et al.'s approximate equation (Eq. (23) in Ref. [25]). We have searched values of ΔG_h and ΔG_r leading to the best fit to the experimental values of f_P at each temperature by trial and error. The solid curves in Figs. 5B and 8 indicate the theoretical results of the best fits for PH3MPS and PRS, respectively, which satisfactorily fit to the experimental g_{abs} for both polysilylenes.

The fitting parameters, ΔG_h and ΔG_r determined for PH3MPS and PRS at each temperature, are compared in Fig. 11. Values of $2\Delta G_h$ are much lower than the thermal energy RT at room temperatures ($\approx$2 kJ/mol). For PH3MPS, $2\Delta G_h$ is almost independent of temperature, indicating that the enthalpic contribution is much larger than the entropic contribution ($2\Delta H_h/RT = 0.029$, $2T\Delta S_h/RT = -0.001$ at -25 °C). On the other hand, for PRS it changes approximately linearly with temperature and furthermore its sign is inverted at ca. 3 °C. Both enthalpic and entropic contributions, $2\Delta H_h/RT$ and $2T\Delta S_h/RT$, are estimated to be ca. 0.20 at the inversion temperature for this polysilylene. The thermal helix-sense inversion of PRS corresponds to this change of the ΔG_h sign. The inversion of the ΔG_h sign will be argued in connection to the internal rotation potential in Section 6. In Fig. 11, the results of a stereospecifically deuterated poly(*n*-hexyl isocyanate) (αPdHIC) in *n*-hexane are also shown by unfilled squares [47]. The values of $2\Delta G_h$ for this polymer is much smaller than PH3MPS and PRS (except in the vicinity of the critical temperature). This is due to weaker chirality of the asymmetric carbon on the side-chains of the deuterated poly(*n*-hexyl isocyanate).

For both PH3MPS and PRS, temperature dependencies of ΔG_Γ are weak and the magnitudes are much larger than $2\Delta G_h$ and also thermal energy ($RT < 3$ kJ/mol). Thus the helix reversal hardly takes place in the polysilylene chains. If the helix reversal is difficult to occur, neighboring repeating units in the chains are forced to take the same helical state, and this correlation induces strong enantiomer selectivity from small $2\Delta G_h$ and also interesting cooperative phenomena in CD for helical homopolymers and copolymers [49]. The sharp sigmoidal changes of g_{abs} (or CD) with temperature and N_0 shown in Figs. 5, 7, and 8 come from this difficulty of the helix reversal in the chains. Values of ΔG_r for a deuterated poly(*n*-hexyl isocyanate) (filled squares in Fig. 11) are even larger than those for PH3MPS and PRS, and the large ΔG_r induce the strong isotope effect on CD or optical activity of the polymer [47].

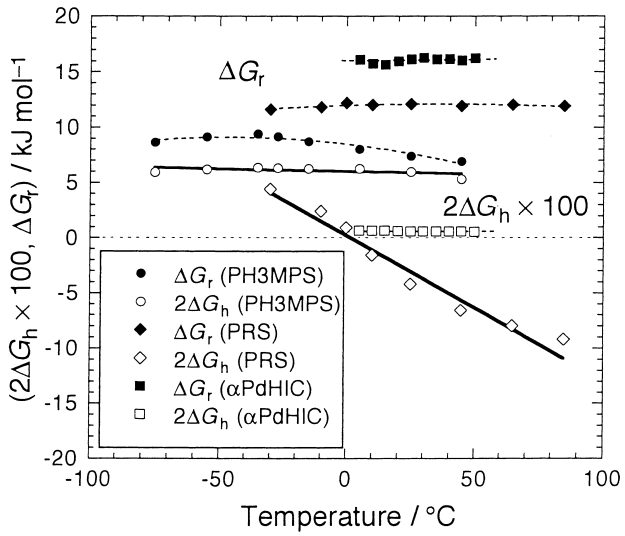

Fig. 11. Thermodynamic parameters ΔG_h and ΔG_Γ determined for PH3MPS (circles) [42] and PRS (diamonds) [9] in isooctane as well as previous results for poly((*R*)-1-deuterio-*n*-hexyl isocyanate) (squares) in *n*-hexane [47].

5. Global conformations [7–10]

5.1. Experimental results

Fig. 12 shows a double-logarithmic plot of $[\eta]M_0$ versus N_0 for four polysilylenes in isooctane, where $[\eta]$ is the intrinsic viscosity, M_0 is the molar mass of the repeating unit and N_0 is degree of polymerization calculated from

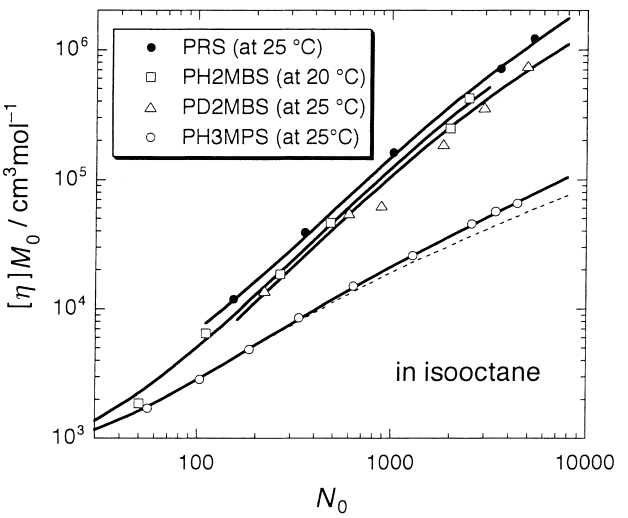

Fig. 12. Double-logarithmic plot of $[\eta]M_0$ versus N_0 for four polysilylenes in isooctane [7–10]. Continuous curves indicate theoretical values for the wormlike cylinder model with parameters listed in Table 1, and the dotted curve corresponds to theoretical values for PH3MPS in the unperturbed state ($B = 0$).

experimental M_w divided by M_0. The quantity $[\eta]M_0$ is a measure of polymer chain size being proportional to the hydrodynamic volume divided by N_0, and we can compare the chain size of different polysilylenes with the same number of main-chain silicon atoms in this figure. The three curves followed by data points for PRS, PH2MBS, and PD2MBS come close each other and the power-law exponent (i.e. the slope of the curves) at intermediate N_0 is ca. 1.3. This exponent is appreciably higher than that expected for flexible polymers, indicating that those polysilylenes possessing considerably high chain rigidity. On the other hand, data points for PH3MPS remarkably deviate downward from the curves for such rigid polysilylenes, and the power-law exponent at high N_0 is as low as 0.75, which is expected for flexible polymers.

As shown in Fig. 13A, $[\eta]$ for high molecular weight PH3MPS samples exhibit strong temperature dependence. The molecular weight dependence of $[\eta]$ is also temperature dependent (cf. Fig. 13B). The power-law exponent increases with decreasing temperature; it reaches to 1.03 at -15 °C in an intermediate molecular weight range, indicating chain stiffening of PH3MPS at low temperatures. For PRS, the temperature dependence of $[\eta]$ was much weaker than that for PH3MPS; the $[\eta]$ increment is only 16% with changing temperature from 25 to -15 °C for a PRS sample ($M_w = 9.1 \times 10^5$) with $[\eta] = 28 \times 10^2$ cm^3/g at 25 °C [9]. Furthermore, the temperature dependence of $[\eta]$ for this PRS sample did not exhibit any singularity around the critical temperature where the helical sense is reversed (cf. Fig. 7). Thus, PRS shows no transition in the global conformation at this temperature.

Fig. 14 compares radii of gyration $\langle S^2\rangle_z^{1/2}$ for the same polysilylenes in the same solvent conditions as in Fig. 12. Here, $\langle S^2\rangle_z^{1/2}$ is another measure of the polymer chain size, and the data given in this figure are consistent with the $[\eta]$ data shown in Fig. 12 with respect to the order of the chain size among the four polysilylenes. The slope of the double-logarithmic plot of $\langle S^2\rangle_z^{1/2}$ versus N_0 is about 0.8 for PH2MBS and PD2MBS, which is another evidence for the non-flexible-chain nature of these polysilylenes. The order of the chain size indicates that the backbone of PRS is slightly stiffer than those of PH2MBS and PD2MBS, and the backbone of PH3MPS is much flexible than the other three polysilylenes.

Fig. 14 also shows $\langle S^2\rangle_z^{1/2}$ data of poly(di-*n*-octyl silylene) (P2OS) and poly(di-*n*-hexyl silylene) (P2HS) samples in solution obtained by Cotts et al. [50]. The data indicates that P2OS and P2HS with linear alkyl side-chains are as flexible as or even more flexible than PH3MPS. It should be however noticed that since the P2OS and P2HS samples used are photodegraded ones without fractionation, their molecular weight distributions are rather broad so that their $\langle S^2\rangle_z^{1/2}$ data may not be competent for quantitative arguments.

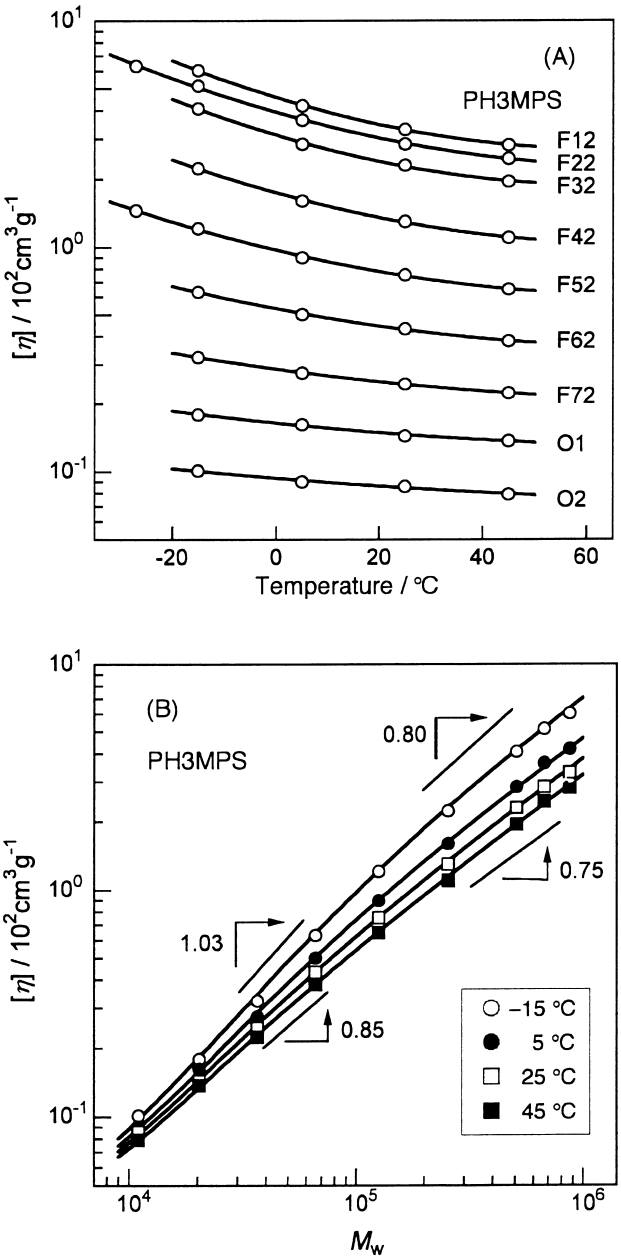

Fig. 13. Temperature and molecular weight dependencies of $[\eta]$ for PH3MPS in isooctane [8]. No. of each sample in Panel A is given in the caption of Fig. 3

5.2. Persistence length

The standard model to express the global chain conformation of rigid or semiflexible polymers is the wormlike-chain model [27,28]. This is a continuous chain model which is characterized in terms of the total contour length L and the persistence length q. For helical polymers, L can be calculated from the pitch h per the repeating unit multiplied by the degree of polymerization N_0, so that h and q are the characteristic parameters of this model chain. Detailed analyses of $[\eta]$ and $\langle S^2\rangle_z^{1/2}$ data for polysilylenes shown in Figs. 12–14 using this model chain were described

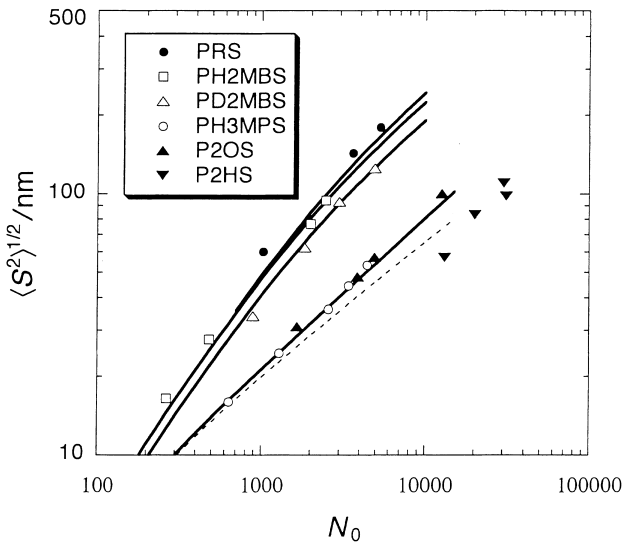

Fig. 14. Double-logarithmic plot of $\langle S^2\rangle_z^{1/2}$ versus N_0 for six polysilylenes, PRS [9], PH2MBS [7], PD2MBS [10], PH3MPS [8], poly(di-*n*-octylsilylene) (P2OS) [50], and poly(di-*n*-hexylsilylene) (P2HS) [50]. Continuous and dotted curves indicate theoretical values for wormlike-chain model with the parameters listed in Table 1 and in the unperturbed state with $B = 0$, respectively.

in previous papers [8,9]. Here we present only results obtained in the previous analyses.

The hydrodynamic calculation of $[\eta]$ needs to specify the polymer chain thickness. When one uses the wormlike-cylinder model [28], the cylinder diameter d is introduced in the theory of $[\eta]$ as an additional parameter. Furthermore, if the polymer chain is flexible enough, we have to consider the intramolecular excluded-volume effect on $[\eta]$ and the radius of gyration. In quasi-two-parameter theories of the excluded volume effect [28], the strength of this effect is expressed in terms of the excluded-volume strength B per unit contour length.

In Fig. 12, solid curves indicate best fits of experimental $[\eta]$ data of the four polysilylenes to the theory of the wormlike cylinder model. For all the polysilylenes, fitting is satisfactory. The dotted curve for PH3MPS is for the unperturbed state where $B = 0$, showing the excluded-volume effect to be appreciable for this polymer at high degrees of polymerization. On the other hand, for the other stiffer polysilylenes, calculations of $[\eta]$ using reasonable values of B do not change the theoretical curves from the unperturbed state, so that this effect is not important in the ranges of N_0 examined. For PH3MPS, $[\eta]$ data at different temperatures shown in Fig. 13 were also analyzed to estimate the wormlike cylinder parameters. Table 1 lists the parameters determined by the fitting.

The radius of gyration $\langle S^2\rangle_z^{1/2}$ for the wormlike chain model is given by [51]

$$\langle S^2\rangle^{1/2} = 2q\left[\frac{1}{6}N - \frac{1}{4} + \frac{1}{4N} - \frac{1}{8N^2}(1 - e^{-2N})\right]^{1/2} \quad (5.1)$$

where N is the number of Kuhn's statistical segments

Table 1
Parameters characterizing polysilylene chain conformations in isooctane

Polymer	Temperature (°C)	h (nm)	q (nm)	d (nm)	B (nm)
PRS [9]	25	0.200	103	3.0	0
PH2MBS [7]	20	0.197	85	2.0	0
PD2MBS [10]	25	0.197	70	1.6	0
PH3MPS [8]	−27	(0.196)[a]	15.4	(1.8)[a]	(1.7)[a]
	−15	0.196	11.9	1.8	1.7
	5	(0.196)[a]	7.7	1.8	1.7
	25	(0.196)[a]	6.1	1.7	1.7
	45	(0.196)[a]	5.0	1.8	1.7

[a] Assumed values.

calculated by $N = hN_0/2q$. Solid curves in Fig. 14 indicate that theoretical values for the polysilylenes calculated by this equation with the wormlike-chain parameters listed in Table 1. The theoretical curves almost fit to the data points, confirming the estimates of the wormlike-chain parameters. The z-average radius of gyration determined by light scattering is however more strongly affected by polydispersity in the molecular weight than $[\eta]$. Thus, slight downward deviations of the theoretical curves may be responsible for this polydispersity effect.

In Table 1, the persistence length q determined for PH2MBS is 14 times as large as that of PH3MPS, despite the location of the methyl group on the side-chain differing only one carbon atom, i.e. β-carbon and γ-carbon. The methyl group on the β-carbon atom of the alkyl side-chain may interact so strongly with neighboring side-chains that the internal rotation about main-chain Si–Si bonds is tightly constrained. On the other hand, such constraints are more or less relieved for PH3MPS because the methyl groups are removed by one carbon atom more from the main-chain. However, the introduction of one more methyl group at the γ-carbon atom in another side-chain of PH3MPS drastically stiffens the polysilylene chain as demonstrated by PRS (see Scheme 1). PRS is even stiffer than aromatic polyamides, polyisocyanates, and double-helical DNA ($q \leq 60$ nm) [52]. Comparing q values of PH2MBS and PD2MBS, the longer alkyl side-chain in PD2MBS does not contribute to the chain stiffness but even makes slightly more flexible the chain. As explained in the next section, the chain stiffness is governed by the steepness of the internal-rotation potential in the main-chain. The slightly shorter q of PD2MBS implies that the longer non-branched alkyl side-chain makes the potential of silicon backbone less steeper. In sum, the potential is affected by the chemical structure of the side-chain of polysilylenes very sensitively and in a complex way.

The persistence length of PH3MPS strongly depends on temperature as seen in Table 1. The temperature dependence of q for PRS was examined by $[\eta]$ data for one PRS sample with a high molecular weight of 9.14×10^5 at different temperatures, with assuming temperature independence of h and d. The analysis indicates that q slightly increases with decreasing temperature but its dependence is weaker than

that for PH3MPS, and it exhibits no significant singularity at the inversion temperature 3 °C (cf. Fig. 16). The temperature dependence of q includes an important information on the internal-rotation potential, which will be discussed in the next section.

In contrast with the persistence length, the pitch h per the repeating unit determined (cf. the third column of Table 1) is ca. 0.2 nm irrespective of the side-chain chemical structure of polysilylenes. This value closely agrees with the pitch (= 0.19 nm) calculated for the 7/3 helix of the polysilylene chain using the standard bond length and bond angle and also with the pitch (0.197 nm) estimated from the X-ray fiber pattern for poly(*n*-pentylsilylene) in crystalline state [53]. Thus, the (most stable) local helical conformation is not essentially affected by the chemical structure of the side-chain nor by environment.

6. Internal potential and helix reversal [24]

In the preceding two sections, we have determined the free-energy difference $2\Delta G_h$ between the P- and M-helical states and the persistence length q of optically active polysilylenes. These two quantities are closely related to the internal rotation potential $E(\tilde{\phi})$ through Eqs. (2.6), (2.7), (2.17), (2.19), and (2.20) as explained in Section 2.

Fig. 15 shows $E(\tilde{\phi})$ about the central bond for oligomers of isotactic (it) and syndiotactic (st) PRS with $N_0 = 31$ terminated with hydrogen, calculated by molecular mechanics with the pcff force field [6]. For both it and st oligomers, $E(\tilde{\phi})$ clearly indicates double minimums at $\tilde{\phi}_0 \approx \pm 20°$, and the minimum at $\tilde{\phi}_0 \approx -20°$ is slightly lower than that at $\tilde{\phi}_0 \approx 20°$. This means that the repeating unit of PRS can take almost enantiomeric right-handed (P) and left-handed (M) helical states and the P state is more stable energetically. The stable rotation angles are close to but

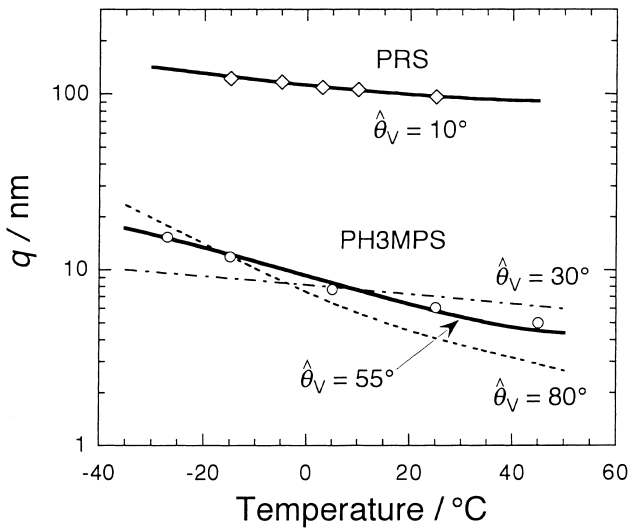

Fig. 16. Comparison between theory and experiment of the persistence length q for PRS and PH3MPS [24].

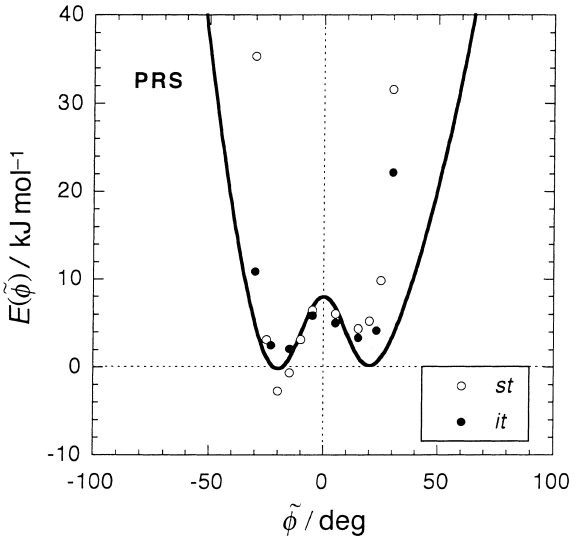

Fig. 15. Internal potentials for PRS calculated by molecular mechanics and obtained by fitting to experimental ΔG_h and q [6,24].

slightly smaller than $\pm 31.3°$ expected for the 7/3 helix of polysilylenes.

In this section, we adopt standard values for the Si–Si bond length b (= 0.234 nm) and the Si–Si–Si bond angle θ (= 111°), as used in Section 2, but the stable internal rotation angles $\tilde{\phi}_0$ to be $\pm 20°$ according to the result of the molecular mechanics in Fig. 15. Furthermore, we assume that the right-handed helix ($\tilde{\phi}_0 = -20°$) is more stable than the left-handed. When we use $\pm 20°$ for the stable $\tilde{\phi}_0$, the helix pitch h per the repeating unit and the kink angle $\hat{\theta}_V$ at the helix reversal becomes 0.192 nm and 11°, respectively, which are not so much different from those for the 7/3 helix (cf. Section 2).

For some polysilylenes, right- and left-handed helices exhibit CD signals at slightly different wavelengths [54], which indicates that pitches of the right- and left-handed helices are not identical for such polysilylenes. However, CD peaks of both PH3MPS [42] and PRS [6,9] in solution is essentially unaltered with changing the right- and left-handed helical population, so that we have no reason for choosing different absolute values of $\tilde{\phi}_0$ for the P- and M-helices for PH3MPS and PRS.

6.1. Determination of parameters

If we expresses $E(\tilde{\phi})$ using Eq. (2.4), we have to determine four adjustable parameters, E_T, $E_{0,P}$ ($= -E_{0,M}$), β_P, and β_M, where the subscripts P and M indicate that parameters are in the negative and positive $\tilde{\phi}$ regions, respectively. Furthermore, Eq. (2.20) of q contains one more unknown parameter $\hat{\theta}_V$; $\langle l \rangle = h\langle l' \rangle$ can be calculated from Eq. (2.15) using ΔG_h and ΔG_r experimentally determined. Thus we have totally five adjustable parameters to calculate $2\Delta G_h$ and q. The magnitude and temperature dependence of ΔG_h are mainly determined by $E_{0,P}$ and the difference $\beta_M - \beta_P$. On the other hand, the magnitude and temperature

dependence of q are predominantly affected by β_P (or β_M) and $\hat{\theta}_V$. Both ΔG_h and q depend on E_T only weakly. Therefore, if E_T is rather arbitrarily chosen, the remaining parameters can be determined by fitting theoretical results to experimental ΔG_h and q.

Referring to the result of the molecular mechanical calculation, we choose 8 kJ/mol as E_T of PRS. Then the other parameters can be determined almost uniquely to fit to experimental ΔG_h and q. The solid curve in Fig. 15 indicates $E(\tilde{\phi})$ calculated by Eq. (2.4) with the parameters determined. This potential provides solid curves for PRS in Figs. 11 and 16 calculated by the theories for ΔG_h and q. In the calculation of q, we have used a value of 10° as $\hat{\theta}_V$. Although not shown, a value of $\hat{\theta}_V$ larger than 20° did not fit to the temperature dependence of q as good as at $\hat{\theta}_V = 10°$. As mentioned above, the two-state approximation gives us $\hat{\theta}_V$ to be 11°, which is consistent with the above estimate for PRS. The value of δ calculated by Eq. (2.21) using the fitting parameters is less than 3.5×10^{-4}, so that $[\eta]$ of the broken and regular wormlike chain models with the same q are indistinguishable.

At present, we have no information on E_T for PH3MPS, but we expect that it may be lower than that for PRS because of less bulky side-chains. If we choose 4 kJ/mol as E_T of PH3MPS, we can determine the remaining parameters almost uniquely to fit to experimental ΔG_h and q. Solid curves for PH3MPS in Figs. 11 and 16 show the fitting results, where we have used a value of 55° as $\hat{\theta}_V$. Uniqueness of the determination of $\hat{\theta}_V$ is demonstrated by dotted and dot-dash curves in Fig. 16; the determination was also independent of the choice of E_T. The value of $\hat{\theta}_V$ determined is much larger than that for PRS as well as the expected value from the two-state approximation. This implies that the PH3MPS chain takes some intermediate conformation at the helix reversal. Although polymer is different, molecular mechanical calculations for polyisocyanates [22,55] demonstrated that two or three repeating units in the vicinity of the helix reversal of a polyisocyanate chain take some intermediate conformations other than the right- nor left-handed helical conformations. The value of δ for PH3MPS was less than 0.156, guaranteeing the identification of q of the broken and regular wormlike chain models.

6.2. Free energy difference between the P- and M-states

To discuss the temperature dependence, we formally divide ΔG_h into the enthalpic and entropic terms as

$$\Delta G_h = \Delta H_h - T\Delta S_h \tag{6.1}$$

where ΔH_h and ΔS_h are the enthalpy and entropy differences between the two states ($\Delta H_h \equiv H_{h,M} - H_{h,P}$; $\Delta S_h \equiv S_{h,M} - S_{h,P}$; cf. Eq. (2.7)). The temperature dependence of ΔG_h is governed by the competition between the enthalpic and entropic terms.

In Fig. 17A, the internal potential for PRS already shown in Fig. 15 (the continuous curve) is plotted against the absolute value of $\tilde{\phi}$ to compare the P- and M-states. The deepness and steepness of $E(\tilde{\phi})$ between the two states are appreciably different for PRS. These two differences provide ΔH_h and ΔS_h, respectively. From the figure, it turns out that both ΔH_h and ΔS_h are positive, and the enthalpic and entropic terms in Eq. (6.1) stabilize the P- and M-helical states, respectively. Therefore, the helix sense inversion observed for PRS can be interpreted as the competition between the enthalpic and entropic contributions or the two kinds of differences in $E(\tilde{\phi})$. For PH3MPS, on the other hand, $E(\tilde{\phi})$ shown in Fig. 17B is almost symmetric, which corresponds to small ΔS_h. As done in a previous paper [9], the relations of the internal potential to ΔH_h and ΔS_h are more intuitively illustrated by using a double square-well potential.

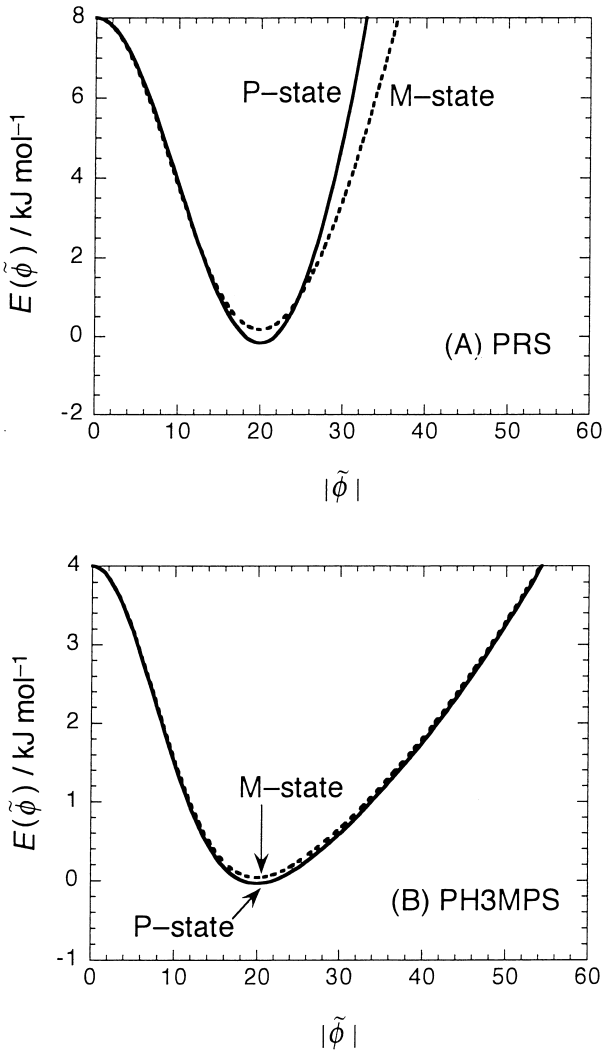

Fig. 17. Comparison of the internal potentials in the P- and M-states; calculated by Eq. (2.4) with the parameters detemined from the ΔG_h and q data; (A) PRS and (B) PH3MPS.

The difference in the shape of $E(\tilde{\phi})$ between PRS and PH3MPS comes from difference in the side-chain chemical structure of the two polymers: both side-chains of PRS

are chiral, so that its internal potential may be more dissymmetric than that of PH3MPS having only one chiral side-chain. Molecular mechanical calculations can explicitly consider the effect of the side-chain structure on $E(\tilde{\phi})$ However, the results of molecular mechanics shown in Fig. 15 slightly exaggerate the dissymmetry of $E(\tilde{\phi})$ for PRS than that determined from ΔG_h and q data. Although the disagreement of $E(\tilde{\phi})$ in the high energy region may not so important in calculations of ΔG_h, ΔG_h is so sensitively dependent on the shape of $E(\tilde{\phi})$ in the vicinity of the minima, that the molecular mechanics cannot precisely predict the thermal inversion of the helix sense of PRS at present.

As demonstrated in Fig. 9, the critical temperature of the helix sense inversion for PRS increases with bulkiness (or the number of branches) of hydrocarbon solvents. This may come from a decrease in ΔS_h with increasing the solvent bulkiness. Although not explicitly considered above, ΔS_h in solution must include the packing or translational entropy of solvent molecules. The easiness of the packing of solvent molecules may be different in the vicinity of polymer chains taking the P- and M-states, but bulky solvent molecules may hardly recognize the chiral environment near the polymer chain. In a previous paper [9], we have formally quantified the solvent dependencies not only of ΔS_h but also of ΔH_h using the double square-well potential to explain the relation between the inversion temperature and the number of branches of solvent molecule.

6.3. Persistence length

As seen from Eq. (2.20), the persistence length q is affected by the three factors, the degree of the torsional fluctuation as well as the frequency and kink angle of the helix reversal. The degree of the torsional fluctuation and the frequency of the helix reversal are expressed in terms of the arithmetic mean of standard deviations $\langle\delta\tilde{\phi}\rangle[\equiv\langle(\tilde{\phi}-\tilde{\phi}_0)^2\rangle_M^{1/2}+\langle(\tilde{\phi}-\tilde{\phi}_0)^2\rangle_P^{1/2})/2]$ calculated from Eq. (2.3) and the arithmetic mean $\langle l\rangle$ of average lengths of a P- and M-sequence given from Eq. (2.15) ($\langle l\rangle = h\langle l'\rangle$), respectively. Fig. 18 compares both quantities for PRS and PH3MPS, calculated from the potentials shown in Fig. 17 and the thermodynamic parameters shown in Fig. 11. It can be seen that both degree of torsional fluctuation and frequency of the helix reversal are higher for PH3MPS than for PRS and furthermore that the temperature dependence of $\langle l\rangle$ is much stronger than that of $\langle\delta\phi\rangle$ for both polysilylenes. As mentioned in subsection 6.1, the kink angle $\hat{\theta}_V$ at the helix reversal is larger for PH3MPS than for PRS. Therefore, all the factors affecting q make the PH3MPS chain more flexible than the PRS chain, which give rise to the remarkable difference in q between PH3MPS and PRS.

The chain flexibility expressed by q^{-1} consists of contributions of the torsional fluctuation and of the helix reversal as indicated by Eq. (2.20). The former contribution is represented by $\langle q_0^{-1}\rangle \equiv f_P q_{0,P^{-1}} + (1-f_P)q_{0,M^{-1}}$. Fig. 19

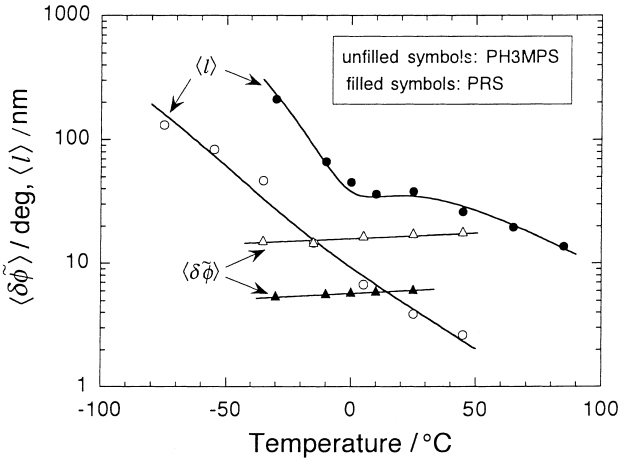

Fig. 18. Temperature dependencies of the arithmetic mean of standard deviations $\langle\delta\phi\rangle$ of the internal rotation angle and the arithmetic mean $\langle l\rangle$ of average lengths of a P- and M-sequence for PRS and PH3MPS [24].

shows the relative contribution of the torsional fluctuation to the chain flexibility, i.e. the ratio of $\langle q_0^{-1}\rangle$ to q^{-1} for PH3MPS and PRS. At low temperatures, $\langle q_0^{-1}\rangle/q^{-1}$ for PH3MPS is large and the chain flexibility is mainly determined by the torsional fluctuation of the internal rotation. On the other hand, the ratio decreases with increasing the temperature, demonstrating that the kink due to the helix reversal plays an important role in the chain flexibility at higher temperature. For PRS, the ratio is almost unity irrespective of temperature, so that the kink due to the helix reversal little contributes to the chain flexibility for this polymer. This comes from long $\langle l\rangle$ and small $\hat{\theta}_V$ for PRS. The minor contribution of the helix reversal to q was also indicated for polyisocyanates theoretically [25] and by viscosity and light scattering experiment [56].

6.4. Absorption spectrum

Fujiki [57] found that the maximum ε_{max} and the half-width fwhm of ultraviolet (UV) absorption spectra of

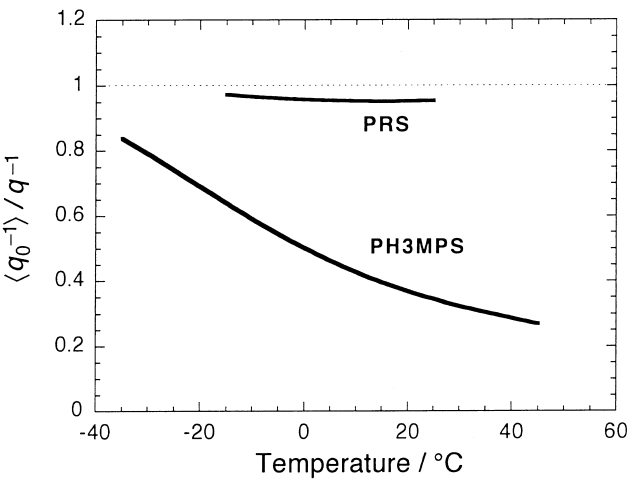

Fig. 19. Ratio of $\langle q_0^{-1}\rangle$ to q^{-1} for PH3MPS and PRS [24].

various polysilylenes closely correlate to their chain stiffness (or the Mark–Houwink–Sakurada exponent). As explained above, the persistence length is related to the torsional fluctuation and the helix reversal, so that electronic state of polysilylene chains may be also correlated to the two disorders of the helical conformation.

Fig. 20 compares ε_{max} and fwhm for PH3MPS [42] and PRS [9] at sufficiently high molecular weights; the data for PH3MPS have been already shown in Fig. 10D. As found by Fujiki, stiffer polysilylene exhibits stronger ε_{max} and narrower fwhm. Furthermore, both quantities strongly depend on temperature. When those ε_{max} and fwhm are plotted against $\langle l \rangle$, data points almost follow universal curves, but we could not obtain composite curves when plotting ε_{max} and fwhm for PRS and PH3MPS at different temperature against $\langle \delta\phi \rangle$, as demonstrated in Fig. 21. Thus, we may say that not the torsional fluctuation but the helix reversal correlates to the electronic state of polysilylene chains.

Abe [38] demonstrated by a quantum mechanical calculation that in conjugated polymeric systems, the fluctuation in the interatomic distance (or the quantum lattice fluctuation) makes the absorption spectrum broader. However, the effect of the helix reversal on the electronic state in conjugated polymers has not been examined yet. The results shown in Fig. 21 indicate that such an examination is quite interesting to reveal the interrelation between the global conformation and optical-electronic properties of polysilylenes.

7. Lyotropic liquid crystallinity [10]

Recently it was found that PD2MBS possesses both lyotropic and thermotropic liquid crystallinity. Fig. 22 shows the molecular weight dependence of the critical concentration c_I where the cholesteric phase begins to appear in isooctane solutions of PD2MBS by circles. It is almost molecular-weight independent in the high M_w region, but sharply increases with decreasing M_w. On the other hand, Watanabe, Kamee, and Fujiki [14] reported a cholesteric phase in PD2MBS in the bulk at M_w higher than 1.8×10^4. The strong M_w dependence of the lyotropic c_I data at low M_w seems to be consistent with their critical molecular weight for the thermotropic liquid crystallinity; the specific volume (corresponding to c_I) of the bulk PD2MBS is about 0.98 cm^3/g.

The scaled particle theory (SPT) for hard wormlike spherocylinders is a standard statistical-mechanical theory used in the quantitative argument of the isotropic-liquid crystal phase equilibrium in stiff polymer solutions [52]. Here we compare the molecular weight dependence of c_I for PD2MBS with this theory. The theory needs three molecular parameters, h, q, and the hard-core diameter d_0 of the cylinder, to calculate c_I. The former two parameters have already determined from $[\eta]$ data in Section 5 (see Table 1).

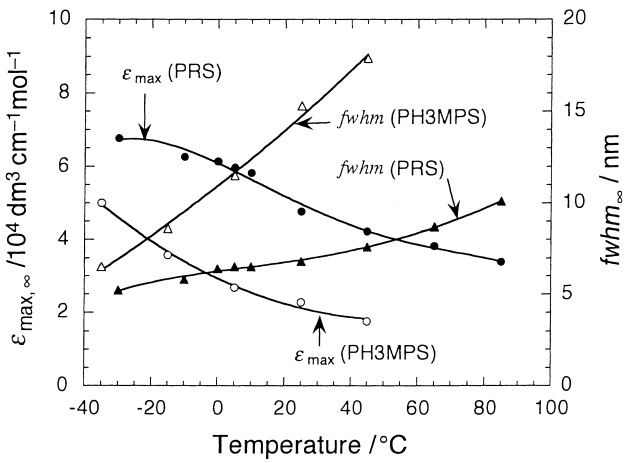

Fig. 20. Temperature dependencies of the maximum ε_{max} and the half-width fwhm of UV absorption spectra for PH3MPS [42] and PRS [9] at sufficiently high molecular weight.

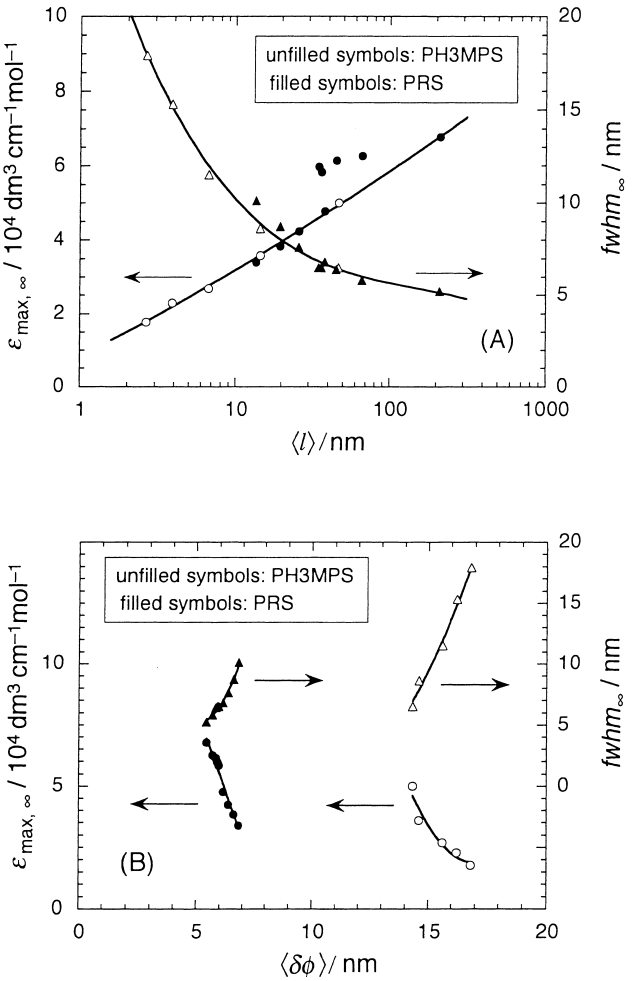

Fig. 21. Plots of the asymptotic maximum ε_{max} and the half-width fwhm of UV absorption spectra against (A) $\langle l \rangle$ and (B) $\langle \delta\phi \rangle$ for PH3MPS and PRS [24].

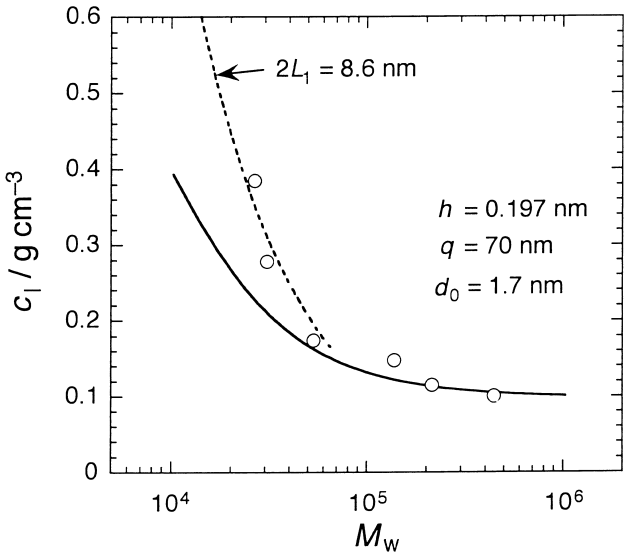

Fig. 22. Molecular weight dependence of the critical concentration c_I where the cholesteric phase begins to appear in isooctane solutions of PD2MBS; circles, experimental data, solid and dotted curves, theoretical values calculated by the scaled particle theory for usual wormlike and tailed-wormlike spherocylinder models, respectively, [10].

The last parameter d_0 may be estimated from the partial specific volume $\bar{v}$ by the equation

$$d_0 = \left(\frac{4\bar{v}M_0}{\pi N_A h}\right)^{1/2} \tag{7.1}$$

where N_A is the Avogadro constant. Using the experimental value for $\bar{v}$ (= 1.107 cm^3/g) and $h = 0.197$ nm, we have a value of 1.7 nm for d_0 of PD2MBS.

The solid curve in Fig. 22 indicates theoretical values of c_I calculated by the SPT. The theory agrees with experimental results at high M_w, but underestimates c_I at $M_w < 5 \times 10^4$. So far, the SPT has successfully predicted c_I of typical stiff polymer solutions. Because the SPT includes higher virial terms in thermodynamic quantities, it is applicable up to high concentrations [52]. The remarkable deviation in the low molecular weight region indicates that some residual conformational entropy remains in the short polysilylene chain in the isotropic phase, which is not taken into account in the theory.

The rigidity of the PD2MBS chain comes from the steric hindrance among neighboring side-chains. In the middle of the main-chain, each side-chain strongly interacts with neighboring side-chains on the both sides along the main-chain, but at the chain end, side-chains may interact each other more loosely, so that the internal rotation in the backbone chain should occur more freely in the vicinity of both chain ends than in the middle of the main-chain. In other words, the PD2MBS chain may be more flexible in the vicinity of the chain ends. At sufficiently high molecular weights, this flexibility effect at the chain ends is neglected, but it may be important with decreasing the molecular weight.

Incorporating the chain end effect, Natsume et al. [10] used the tailed wormlike chain model to calculate c_I. This model chain consists of three portions, the wormlike-chain middle portion 2 and the freely jointed-chain end portions 1 and 3 of which contour lengths are denoted as L_2, L_1, and L_3, respectively. If the contour length of the end portions $2L_1$(= $L_1 + L_3$) is chosen to be 8.6 nm, the SPT for this model chain provides c_I indicated by dotted curve in Fig. 22, which are in good agreements with experimental results in the low M_w region. The representation of the end portions by the freely jointed chain is a little bit so crude that we do not argue the physical significance of the contour length of the end portions obtained. It is noted that the flexibility effect at the chain ends appreciably affects the isotropic-liquid crystal phase equilibrium, but it does not essentially contribute to the intrinsic viscosity as demonstrated by Natsume et al. Therefore, the wormlike chain analysis in Section 5.2 is hardly affected by this effect for all polysilylenes.

References

[1] Miller RD, Michl J. Chem Rev 1989;89:1359–410.
[2] Jones RG, Ando W, Chojnowski J. Silicon-containing polymers. Dordrecht: Kluwer Academic Publishers; 2000.
[3] Fujiki M. Macromol Rapid Commun 2001;22:539–63.
[4] Fujiki M, Koe JR, Terao K, T S, Teramoto A, Watanabe J. Polym J 2003;35:297–344.
[5] Michl J, West R. Silicon-containing polymers. In: Jones RG, Ando W, Chojnowski J, editors. Electronic structure and spectroscopy of polysilanes. Dordrecht: Kluwer Academic Publishers; 2000.
[6] Fujiki M, Koe JR, Motonaga M, Nakashima H, Terao K, Teramoto A. J Am Chem Soc 2001;123:6253–61.
[7] Terao K, Terao Y, Teramoto A, Nakamura N, Terakawa I, Sato T, Fujiki M. Macromolecules 2001;34:2682–5.
[8] Terao K, Terao Y, Teramoto A, Nakamura N, Fujiki M, Sato T. Macromolecules 2001;34:4519–25.
[9] Teramoto A, Terao K, Terao Y, Nakamura N, Sato T, Fujiki M. J Am Chem Soc 2001;123:12303–10.
[10] Natsume T, Wu L, Sato T, Terao K, Teramoto A, Fujiki M. Macromolecules 2001;34:7899–904.
[11] Nakano T, Okamoto Y. Chem Rev 2001;101:4013.
[12] Nakamura Y, Norisuye T. Polym J 2001;33:874–8.
[13] Wintermantel M, Gerle M, Fischer K, Schmidt M, Wataoka I, Urakawa H, Kajiwara K, Tsukahara Y. Macromolecules 1996;29:978–83.
[14] Watanabe J, Kamee H, Fujiki M. Polym J 2001;33:495–7.
[15] Donald AM, Windle AH. Liquid crystalline polymers. Cambridge: Cambridge University Press; 1992.
[16] Tsukahara Y, Ohta Y, Senoo K. Polymer 1995;36:3413–6.
[17] Wintermantel M, Fischer K, Gerle M, Ries R, Schmidt M, Kajiwara K, Urakawa H, Wataoka I. Angew Chem 1995;107:1606–8.
[18] Maeno K, Nakamura Y, Terao K, Sato T, Norisuye T. Kobunshi Ronbunshu 1999;56:254–9.
[19] Furukawa S, Takeuchi K, Shimana M. J Phys: Condens Matter 1994;6:11007–14.
[20] Bates TW. Trans Faraday Soc 1967;63:1825–34.
[21] Tadokoro H. Structure of crystalline polymers. Malabar, FL: Robert E Krieger Publishing; 1990.
[22] Lifson S, Felder CE, Green MM. Macromolecules 1992;25:4142–8.
[23] Cook R. Macromolecules 1987;20:1961–4.

[24] Sato T, Terao K, Teramoto A, Fujiki M. Macromolecules 2002;35: 2141–8.
[25] Lifson S, Andreola C, Peterson NC, Green MM. J Am Chem Soc 1989;111:8850–8.
[26] Volkenstein MV. Configurational statistics of polymer chains. New York: Interscience Publishers; 1963.
[27] Yamakawa H. Modern theory of polymer solutions. New York: Harper and Row; 1971.
[28] Yamakawa H. Helical wormlike chains in polymer solutions. Berlin: Springer; 1997.
[29] Mansfield ML. Macromolecules 1986;19:854–9.
[30] Koyama R. J Phys Soc Jpn 1973;34:1029–38.
[31] Murakami H, Norisuye T, Fujita H. Macromolecules 1980;13: 345–52.
[32] Kuwata M, Murakami H, Norisuye T, Fujita H. Macromolecules 1984;17:2731–4.
[33] Norisuye T, Tsuboi A, Teramoto A. Polym J 1996;28:357–61.
[34] Takeda K, Shiraishi K, Matsumoto N. J Am Chem Soc 1990;112: 5043–52.
[35] Hasegawa T, Iwasa Y, Sunamura H, Koda T, Tokura Y, Tachibana H, Matsumoto M, Abe S. Phys Rev Lett 1992;69:668–71.
[36] Hasegawa T, Iwasa Y, Koda T, Kishida H, Tokura Y, Wada S, Tashiro H, Tachibana H, Matsumoto M. Phys Rev B 1996;54:11365–74.
[37] Abe S, Schreiber M, Su W-P. Chem Phys Lett 1992;192:425–9.
[38] Abe S. Prog Theor Phys 1993;113(Suppl):83–90.
[39] Abe S, Schreiber M, Su W-P, Yu J. Mol Cryst Liq Cryst 1992;217: 1–6.
[40] Schreiber M, Abe S. Synth Meth 1993;55:50–5.
[41] Natsume T. MS Thesis, Osaka University, 2001
[42] Terao K, Terao Y, Teramoto A, Nakamura N, Fujiki M, Sato T. Macromolecules 2001;34:6519–25.
[43] Berova N, Nakanishi K, Woody RW. Circular doichroism: pronciples and applications. New York: Wiley–VCH; 2000.
[44] Rodger A, Nordén B. Circular dichroism and linear dichroism. Oxford: Oxford University Press; 1997.
[45] Moffitt W, Moscowitz A. J Chem Phys 1959;30:648–60.
[46] Green MM, Andreola C, Munoz B, Reidy MP, Zero K. J Am Chem Soc 1988;110:4063.
[47] Okamoto N, Gu H, Nakamura Y, Sato T, Teramoto A. Macromolecules 1996;29:2878–84.
[48] Gu H, Nakamura Y, Sato T, Teramoto A, Green MM, Andreola C. Macromolecules 1995;28:1016–24.
[49] Sato T, Terao K, Teramoto A, Fujiki M. Macromolecules 2002;35: 5355–7.
[50] Cotts PM, Miller RD, Trefonas III PT, West R, Fickes GN. Macromolecules 1987;20:1046–52.
[51] Benoit H, Doty PM. J Phys Chem 1953;57:958.
[52] Sato T, Teramoto A. Adv Polym Sci 1996;126:85–216.
[53] Miller RD, Farmer BL, Fleming W, Sooriyakumaran R, Rabolt JF. J Am Chem Soc 1987;109:2509–10.
[54] Fujiki M. J Am Chem Soc 1994;116:11976.
[55] Young JA, Cook RC. Macromolecules 2001;34:3646–53.
[56] Gu H, Nakamura Y, Sato T, Teramoto A, Green MM, Andreola C. Polymer 1999;40:849–56.
[57] Fujiki M. J Am Chem Soc 1996;118:7424–5.

Takahiro Sato was born in Osaka in 1957, graduated from the Department of Macromolecular Science, Faculty of Science, Osaka University 1980, and received his PhD from Osaka University in 1985. He started working in 1985 as a guest scientist at National Bureau of Standards (now National Institute of Standards and Technology) in the United States, and then joined the Department of Macromolecular Science, Osaka University as a research associate in 1987. He promoted to an Associate Professor in 1996 and a Full Professor in 2002 at Osaka University. His major research field is polymer solution properties, and he is now interested in the interrelations between the polymer interactions and various solution properties, e.g. rheological properties, liquid-crystalline structures, and phase or aggregation behavior.

Ken Terao was born in 1971 (Osaka, Japan), graduated from the Department of Macromolecular Science, Osaka University in 1994, and received his Dr of Science degree from Osaka University in 1999. He studied solution properties of regular-branched polymers during his doctoral course research. From 1999 to 2001, he worked at Ritsumeikan University for Japan Science and Technology Corporation (JST) as a researcher and studied helical structures of optically active polysilanes in solution. In 2001, he joined the Department of Biological and Chemical Engineering, Gunma University as an Assistant Professor. His research interests include solution properties of polymers and synthesis and properties of microcapsules.

Akio Teramoto was born in 1933 (Ishikawa, Japan), received his BS in 1956 and PhD in 1965 (Kyoto University). He worked at Osaka University from 1961 to 1997, where he is Professor Emeritus, and is currently Chair Professor at Ritsumeikan University and reaearch staff of CREST of Japan Science and Technology Corporation. He received the Award of the Society of Polymer Science, Japan (SPSJ) in 1974 and the SPSJ Award for Outstanding Achievement in Polymer Science and Technology in 1995. His research interests include chain conformations and conformational transitions in dilute solution of polypeptides, polyisocyanates, polysaccharides, and polysilylenes, thermodynamics and dynamics of stiff polymer solutions including polymer liquid crystals, and water structures in aqueous biopolymer solutions.

Michiya Fujiki was born in Fukuoka, Japan, in 1954. He received BS and MS degrees in chemistry of organic synthesis from Kyushu University, Fukuoka, Japan in 1976 and 1978, respectively, and received his PhD degree from Kyushu University, Fukuoka,Japan, in 1993. Since 1978, he has worked for Nippon Telegraph and telephone Cooperation (NTT). From 1978 to 1982, he studied low-loss optical plastic fibers and from 1983 to 1987, he studied the preparation and thin film properties of semiconducting phthalocyanine derivatives. In 1987, he joined the Basic Research laboratories of NTT. From 1987 to 1991, he initiated the study on synthesis and photophysical properties of polysilylenes bearing aryl groups. From 1992 to 2002, he has been engaged in the study of synthesis and photophysical properties of optically active polysilanes and π-conjugating polymers. Since May 2002, he is a full professor at advanced polymer science laboratory, graduate school of materials science, Nara institute of science and technology (NAIST). Professor Fujiki is a member of the Society of Polymer Science Japan, the Chemical Society of Japan, the Society of Silicon Chemistry Japan, and the American Chemical Society.